2017 Annual Report

Institute for Biophysics

Department of Nanobiotechnology

University of Natural Resources and Life Sciences Vienna

2017 ANNUAL REPORT: INSTITUTE FOR BIOPHYSICS (DNBT-BOKU VIENNA)

Foreword

2017. Fifth annual report. The last annual report before we change to bi-annual ones. This has advantages and disadvantages. We might lose track on short projects but the reports will scientifically be more round.

2017 has (again) been a good year. It seems better than 2016, at least from the metrics point of view: 19 articles and 20 contributions to conferences (workshops and seminars). The third party money is still in good numbers (with Notburga Gierlinger as main actress) and we have increased the number of examined students in the Biotechnology MSc (which is still low but with lectures at master level we cannot expect a better deal; teaching is an issue that would need a couple of pages).

A highlight of the year has been the successful Habilitation of Notburga Gierlinger (in Physical and Chemical Biology), which followed to her promotion to Associate Professor (A2 position). I am happy to see that her group is fully integrated in the institute and the department (scientifically and socially). This is important since their research topics and experimental techniques are unique for DNBT. From our part I am satisfied to see that biomaterials mechanics and force spectroscopy (in general) is already established as research line.

The Biophysics Summer School was also an interesting event (this year we invited Assoc. Prof. Radostina Georgieva). Such "party" is important to know and discuss "our science" as well as to get to know each other better. In fact, it gives me a global picture of what is going on and help us to strength the collaborations inside the institute. Even if we do not repeat place and time, we will try to organize one every year.
Remake from 2016 that is still valid: i) we are still managing laboratories that are constantly used by DNBT coworkers and "external" researches, ii) we are participating in BOKU commissions concerning leadership, teaching, research and ethical matters (DLK, DokStuko, FachStuko, Forschungsprecher, ethics platform). No space, no time for complaining about the burocracy involving the Head of Department job (which could end in December 2018; we will see).
During 2017, we have been "34" people between members and visitors. But more impressive for me is the number of students who were performing experiments in our labs: 11 PhD, 5 MSc and 2 BSc. Among them, 8 came from abroad (or other Austrian institutions) to work with us. This is a success.
A very nice experience was to have Marti Duocastella as visiting professor. He lectured on basic optics. He did an outstanding job. I hope he will visit us again because I think that we can learn many things from him. I like having visitors around. This is also the way I started my career. Therefore, we will continue to invite (with pleasure) researches and students from other countries.

As always, I would like to thank all the people who made this report possible, and wish all the best to the coworkers who left the institute to continue a professional career somewhere else. Here I would like to remember Claudia König, the first *Lehrling* that we all have "educated".

Thank you (and good night).

José L. Toca-Herrera

Institute members and visitors – 2017

- Univ. Prof. Dr. José L. Toca-Herrera (director)
- Ao. Univ. Prof. Dr. Dietmar Pum (deputy director)
- Assoc. Prof. Dr. Notburga Gierlinger (group leader)
- O. Univ. Prof. em. Uwe B. Sleytr (emeritus, former director)
- Dr. Andreas Breitwieser (post-doctoral research assistant)
- Dr. Marti Duocastella (ITT, Italy)
- Dr. Jagoba J. Iturri (univ. assistant)
- Dr. Itziar Otazo (tech. assistant)
- Dr. Sudarat Tharad (univ. assistant)
- Dr. Med. Michael Handler (PhD student, collaboration with Sports Univ. Innsbruck, Austria)
- Mag. Amsatou Andorfer-Sarr (techn. assistant)
- MSc. Peter Bock (PhD student)
- MSc. Martin Feldhofer (PhD student)
- Mag. Jacqueline Friedmann (tech. assistant)
- MSc. Elham Ghorbani Gorji (PhD student, collaboration with Inst. Food Sci. - BOKU)
- MSc Violetta Golebiewska (PhD student)
- MSc. Sonia Krysiak (PhD student, AGH-Krakow, Poland)
- MSc. Alberto Moreno-Cencerrado (PhD student)
- MSc. Batirtze Prats Mateu (PhD student)
- MSc Eva Sanchez (PhD student, collaboration with University of the Basque Country, Spain)
- MSc. Nadia Sasani (PhD student)
- MSc. Maria Sumarokova (PhD student, Erasmus Mundus Iamonet Program)
- MSc Carmen Teixeira (PhD student, collaboration with Lincoln University, New Zealand)
- MSc Öyku Üzulmez (techn. assistant)
- MSc. Zuzana Vanekova (PhD-ÖEAD student, Comenius University in Bratislava, Slovakia)
- MSc. Nannan Xiao (PhD student)
- BSc. Damir Begic (MSc – CEEPUS student, University of Sarajevo, Bosnia-Herzegovina)
- BSc. Leif Löher (MSc Erasmus student, TU-Berlin, Germany)
- BSc. Piet Mitjen (MSc-Erasmus student, Gent University, Belgien)
- BSc. Kevin Saabe (MSc-Erasmus student, Gent University, Belgien)
- BSc. Andreas Weber (MSc student)
- Michael Pilgerstorfer (BSc student)
- Claudia König (apprentice)
- Iris Strube (apprentice)

Studying the influence of microtubules on the mechanical properties of endothelial cells via atomic force microscopy and fluorescence microscopy

Andreas Weber[1], Jagoba Iturri[1], Jose L. Toca-Herrera[1]
(1) Institute for Biophysics, Department for Nanobiotechnology, University of Natural Resources and Life Sciences Vienna

Aim/Objective

The mechanical properties of cells play an essential role in cell differentiation, communication between cells, proliferation and many other cellular processes. Variations in mechanical properties are indicators of those changes in cells. Among other components the cytoskeleton plays a major role for those mechanical properties and other cell functions. The three most abundant features of the cytoskeleton are the actin filaments, the intermediary filaments and the microtubules. From these, microtubules play main roles in mitosis, mechanical support, intercellular transport and cellular motility as well as force generation. The influence exerted by the cytoskeletal elements on cellular mechanics has been studied techniques in recent years. A suitable methodology is the combination of atomic force microscopy (AFM) with optical or fluorescence microscopy (FM). It enables the correlation of force curves measured on different position of the cells with the underlying cellular features. Together with thorough analysis of e.g. the elastic and viscous response of the cell the influence of components on the mechanical properties can be elucidated. The aim of the present work is to study the influence of microtubules on cell mechanics with a combination of AFM and FM methods. In addition, the impact of interrupting the dynamic growth of microtubules by addition of colchicine, a microtubule depolymerizing drug, will be tested as function of time and concentration. We will study the apparent Young's Modulus, relaxation times, compressive moduli and viscosity during the pause part and adhesive forces between the tip and the cell during retraction. Statistical analysis will be used to furthermore study if the changes present are of significance.

Results

Preliminary data evaluation showed how disruption of the microtubular network indeed has an impact on different mechanical properties of the studied HUVEC cells. The data generated for an incubation time of up to 80 minutes with a colchicine concentration of 2 mM shows that for nearly all the evaluated mechanical properties (Young's Modulus, relaxation times, position of rupture events and rupture forces during retracting, …) there are shifts in the parameters and in their distributions. Using different fittings and statistical analysis the significance of these changes can be evaluated. It's important to note that because of the diffusion limit of colchicine and the kinetics of its interaction with the microtubules changes in cellular properties are not to be expected immediately after adding the drug. Therefore, studies with longer incubation times and a time-study of the cells with fluorescence microscopy after dyeing the microtubules are necessary to generate enough data to conclude the significance of the existing present changes of cellular properties.

Acknowledgments

This work was partially funded by the FWF.

Polymer brushes as 3-D template for assembly of hierarchical structures

Jacqueline Friedmann[1], Michael Pilgerstorfer[1], Jagoba Iturri[1], Jose L. Toca-Herrera[1]
(1) Institute for Biophysics, Department for Nanobiotechnology, University of Natural Resources and Life Sciences Vienna

Aim/Objective

Polymer brushes are surface coatings consisting of polymeric chains tethered to a surface one end attached to the surface the other end remaining free and exposed to the environment. Depending on the choice of monomeric units forming the polymer chains, these can be controlled in matters of length and charge and might also show conformational changes upon external stimuli, which allows a broad variety of applications. Different examples of this assemblies would be: charge-sensitive (PMETAC, PSPM), temperature responsive (PNIPAM) or additional brush-like structures with other particular surface properties (PEA, PHEMA,…).
Furthermore polymer brushes can be grown following defined patterns by printing the polymerisation initiator, or alternatively a blocking agent by using microstructured PDMS stamps prior the polymer growth. Due to their 3D-like component (caused by the perpendicular stretching from the surface) brushes can be regarded as suitable supports for the binding of additional materials in order to build more complex supramolecular entities. Therefore, the use of particles, polymers or proteins can derive into a full bunch of attractive designs with materials or biologically related applications.

Results

1. Brush patterning

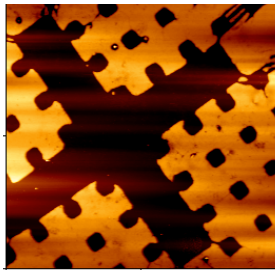

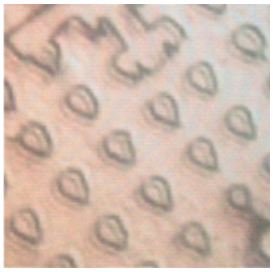

Printing positive pattern:

printing the polymerisation initiator (ATRP) in pattern prior the polymer chain growth of PMETAC (positively charged) or PSPM (negatively charged) on an activated gold surface.

Figure 1. AFM height image (left) size 100µm x 100µm and optical microscope image (right), dropsize ~20µm show positively patterned PSPM brushes

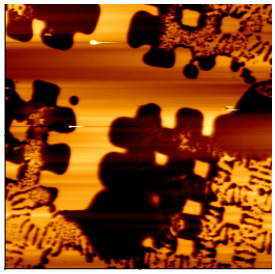

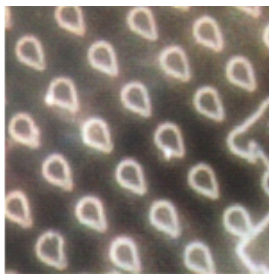

Printing negative pattern (=blocking):

printing a blocking agent (HS-(EG)$_3$-OH) prior ATRP binding and the polymer chain growth on an activated gold surface.

Figure 2. AFM height image (left) size 100µm x 100µm and optical microscope image (right), dropsize ~20µm show negatively patterned PSPM brushes

2. Directed adsorption of capsules on charged patterned polymer brushes

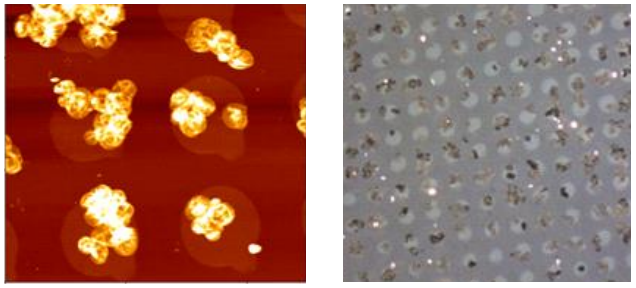

Figure 3. AFM height image (left) size 50µm x 50µm and optical microscope image (right), taken with 20x objective show negatively charged PSPM brush-pillars with positively charged $CaCO_3$/PAH-capsules (binding only to the brush pillars)

Conclusions

Polymer brushes show their versatility for several applications like trapping particles and capsules (drug delivery system) or even cells with subsequent controlled release, furthermore as a preliminary coating for following adsorptions of polyelectrolytes or proteins or as a cell mimicking layer.

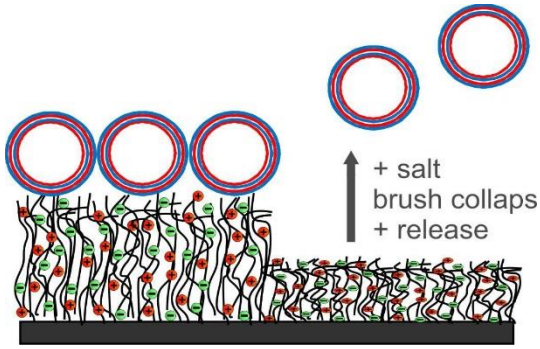

Figure 4. Schematic drawing of the polymer brush drug delivery system with controlled particle release

Insights into microchemistry of supercooling spruce bud tissues

Edith Kuprian[1], Gilbert Neuner[1] and Notburga Gierlinger[2]
(1) University of Innsbruck, Institute of Botany, Unit Functional Plant Biology, Sternwartestr. 15, 6020 Innsbruck, Austria
(2) Institute for Biophysics, Department of Nanobiotechnology, BOKU-University of Natural Resources and Life Sciences, Muthgasse 11/II, 1190 Vienna, Austria

Aims/Objectives

For a better understanding how a plant designs tissues for supercooling, Raman imaging was applied on ice barrier tissues of spruce buds.

Background

The overwintering vegetative bud primordia of *Picea abies* trees manage to stay ice free by a mechanism termed supercooling and by this survive frosts down to -40 °C. A complex architecture that insulates the bud primordia tissue from potential ice entrance and densely packed and highly water repellent bud scale architecture was recognized. Two dimensional freezing patterns monitored by infrared video thermography revealed that the initial ice wave at -10,6 °C in the stem stops, where the xylem tissue ends, and, only a second later, ice spread into the intercellular spaces of bud scales and subtending tissues and stopped below the bud primordia. Intrinsic ice nucleation is impeded by a bowl like ice barrier tissue formed by the crown and a similarly designed tissue belonging to the innermost bud scales. To get new insights into the supercooling design of plants, this bowl like ice barrier tissue was investigated using the Raman imaging approach to reveal chemistry in context with the microstructure.

Results

After acquiring in the region of interest (Fig. 1A, white rectangle, 50x250µm) Raman spectra using the 785nm laser line (100mW) Raman images have been calculated by integrating selected wavenumber regions. The black white image shows all organic structures (Fig. 1B)by integrating a broad region from 1056 to 1137 cm^{-1}, assigned to mainly to C-C and C-O-stretching vibrations of carbohydrates. Integrating selectively the for cellulose typical 380 cm^{-1} band only the cell wall is highlighted (Fig. 1B, red image) and by focusing on the pectin characteristic band at 854 cm^{-} the pectin distribution is followed (Fig. 1B, pink image). While cellulose is restricted to the cell wall itself, pectin is found in the cell wall and to an even higher extent as a glue between the cells. An average spectrum extracted from the investigated region shows high contribution of pectin (typical strong 854 cm^{-1} band) and to less extent cellulose signals (typical strong 1096 cm^{-1} band) (Fig. 1C, black spectrum). The thick walls of the crown as well as the thinner walls towards the primordium are thus revealed as pectin rich cellulosic cell walls. Furthermore contributions from proteins are suggested by the 1655 cm^{-1} band (amide I stretching vibration of C=O). By integrating the starch specific band at 477 cm^{-1} reveals that especially the thinner cells near the primordium contain starch (Fig. 1B, blue image). Extracting a single spectrum from one of those regions (white cross) shows clearly the starch contribution with the typically very strong 477 cm^{-1} band (assigned to C-C-C bending and C-O torsion) as well as strong bands at 859 cm^{-1}, 939 cm^{-1}, 1089 cm^{-1}, 1122 cm^{-1}, 1337 cm^{-1} and 1455 cm^{-1} (Fig. 1C, blue spectrum). The sharp band at 1004 cm-1 points furthermore to phenylalanine (proteins). The distribution of proteins was in a next step visualized

by integrating the amid I region from 1523 cm^{-1} to 1700 cm^{-1} Fig. 1B, green image). Clearly proteins are lining the cell walls towards the lumen and almost filling up some cells. An extracted (white cross) representative single spectrum shows typical protein bands (Fig. 1C, green spectrum) and confirms that proteins are partly filling up the cells in the investigated region (Fig. 1B, green image).

Conclusions

The detected high carbohydrate content of the thick supercooling cell walls contributes to freezing tolerance. Pectins reduce the pore size diameter in cell walls and by this cell walls become impermeable for ice as water in small pores freezes at successively lower temperatures. Furthermore the peculiar distribution pattern of proteins in the cytosol will enhance antifreezing properties.

Acknowledgement

Austrian Science Fund (FWF) project P23681-B16 and START-project (Y-728-B16]

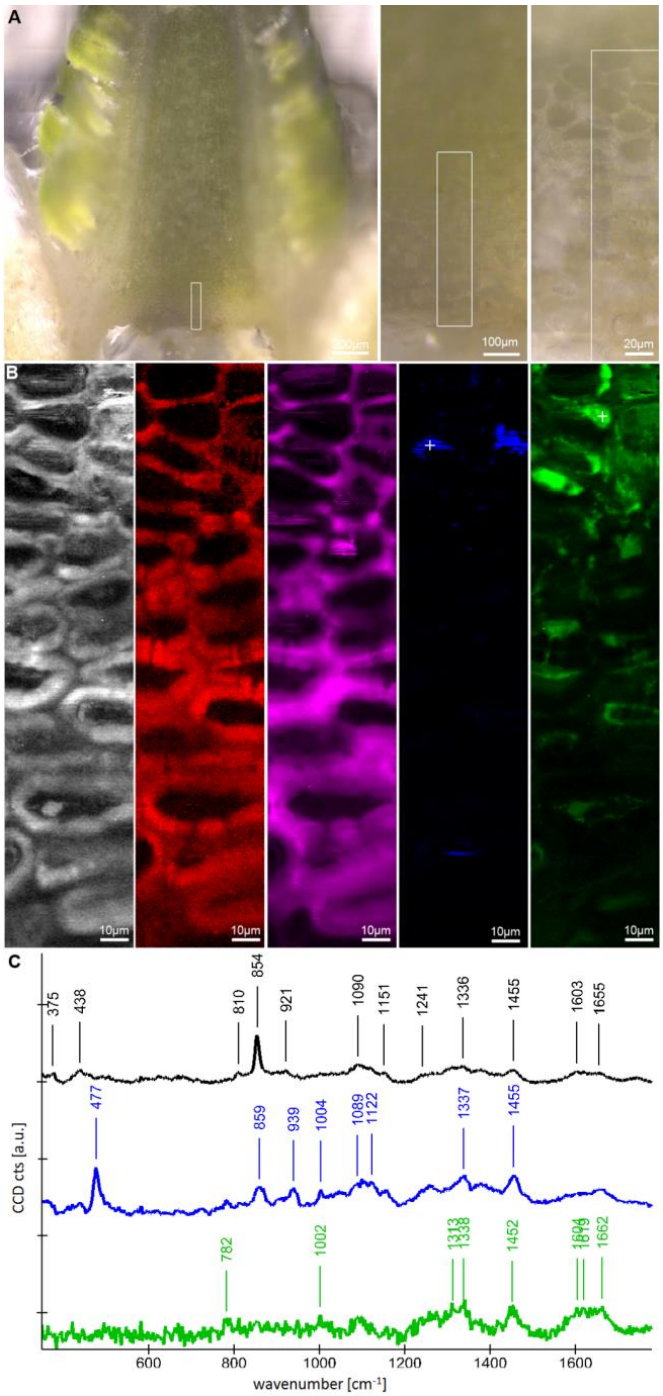

Figure 1. Raman imaging on a micro-cut spruce bud: The region of interest was restricted to the crown tissue as marked in the light microscopic overview images (A). After spectra acquisition Raman images (B) are calculated by integrating from 1056 to 1137 cm^{-1} (black and white, all structures), 370 to 385 (red, cellulose), 838 to 868 cm^{-1} (pink, pectin), 462 to 500 cm^{-1} (blue, starch) and 1523- 1700 (green, protein). Extracted Raman spectra (C) reveal details on the molecular structure of the whole investigated region (black spectrum) and the starch (blue spectrum) and protein (green spectrum) rich deposits. White crosses in the Raman images mark the position of the extracted starch and protein spectrum.

Leather wood: exceptional wood microchemistry revealed by Raman imaging

Yaseen Mottiar[1], Nadia Sasani[2] and Notburga Gierlinger[2]
(1) Institute for Biologically Inspired Materials, Department of Nanobiotechnology, BOKU-University of Natural Resources and Life Sciences, Muthgasse 11/II, 1190 Vienna, Austria
(2) Institute of Biophysics, Department of Nanobiotechnology, BOKU-University of Natural Resources and Life Sciences, Muthgasse 11/II, 1190 Vienna, Austria

Aims/Objectives

New insights into microchemistry of leatherwood to explain the unusual high flexibility of leatherwood.

Background

Eastern leatherwood (*Dirca palustris* L.), also known as moosewood, wicopy and, in French, bois de plomb), is a woody shrub found sporadically across eastern North America in rich, mesic soils of hardwood and mixed forests (Zasada, 2008). These leatherwood stems are exceptionally pliable and flexible such that one can easily tie a twig into a knot without it snapping. Some authors have suggested that poor lignification is the cause of leatherwood´s flexibility, others have pointed to the unusual patterning of cells in leatherwood stems.

Results

Raman imaging was able to reveal unusal microchemistry of leatherwood. The low lignin content could be confirmed in the cell wall, whereby water transporting xylem vessels showed higher lignin contents compared to vasicentric tracheids and libriform fibres (Fig. 1A). Surprisingly no lignin was visualized by the band integration of the 1600 cm^{-1} band between the cells, in the compound middle lamella and cell corners (Fig. 1A). This was surprising as usually lignified wooden cell walls are always glued together by lignin and lignification is even reported to start in the cell corners. Instead pectin is visualised by integrating the marker band at 856 cm^{-1} clearly in the cell corners between the vessels and fibers, beside in the primary cell wall of ray parenchyma walls arranged in the specific pattern of tangential and radial rows (Fig. 1B). Integrating the cellulose orientation sensitive 1096cm^{-1} band highlights the vessel and tracheid walls in the laser polarisation direction (x-axix), an indication for rather high microfibril angle within these secondary cell walls.

Conclusions

Low lignin content and the pectin as a glue between the cells as well as the high microfibril angle are all characteristic features which add flexibility to this wooden tissue.

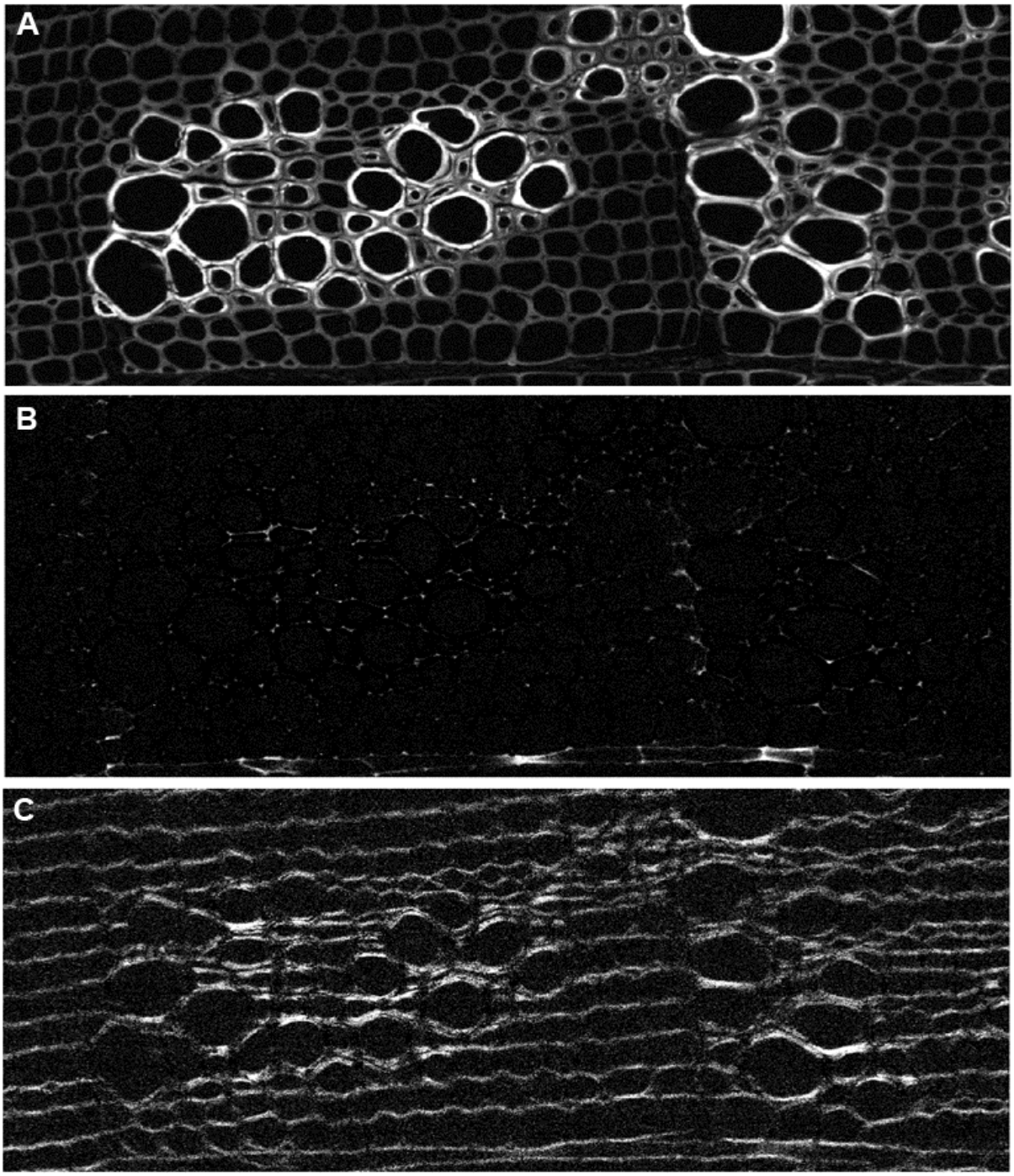

Figure 2. Raman images of a microsection of leatherwood based on band integration of A) 1600 cm^{-1} band to show changes in lignin amount, B) 856 cm^{-1} to reveal pectin distribution and C) the orientation sensitive 1096 cm^{-1} band to draw conclusions on the cellulose microfibril angle.

S-layer directed nanoscale fluid mechanics

Dietmar Pum[1], Andreas Breitwieser[1], Jose Luis Toca-Herrera[1], Uwe B. Sleytr[1]
(1) Institute for Biologically Inspired Materials, Department of Nanobiotechnology, BOKU-University of Natural Resources and Life Sciences, Muthgasse 11/II, 1190 Vienna, Austria

Aim/Objective

The main objectives of this research proposal are the detailed investigation of the anti-fouling and the hydrodynamic surface properties of S-layers. We assume that the S-layer modifies the structure of the first "locked-in" water layer(s) and, in this way, makes it to a liquid-repellent and slippery surface.

Anti-fouling properties of S-layers

Crystalline bacterial cell surface layer proteins (S-layer proteins) represent the outermost cell envelope component in a broad range of prokaryotes (bacteria and archaea), and are one of the most abundant biopolymers on earth. S-layers are isoporous protein mesh works with unit cell sizes in the range of 3 to 30 nm, thicknesses of 5 to 10 nm (up to 70 nm in archaea), and pore sizes of 2 to 8 nm. A broad range of specific functions of S-layers has been studied over the last decades (e.g. acting as molecular sieves, determination of cell shape, etc.) but their role in the interaction with water, either standing or in cross-flow, has still to be investigated.

The main objectives of this research project are the detailed investigation of the anti-fouling properties and the flow resistance of S-layers as benefits for bacterial cells. During the first project year we observed that dried S-layers show hydrophobic while wet lattices – covered with locked-in water layers - reveal hydrophilic surface characteristics. In this context, BslA, a bacterial hydrophobin, which forms extremely hydrophobic coatings in nature, was chosen to be displayed on the S-layer surface to enhance its hydrophobicity. Therefore, a recombinant S-layer - hydrophobin fusion protein rSbpA BslA was genetically engineered and successfully expressed in *E. coli.* After purification with gel chromatography the capability to form recrystallization products was investigated by AFM and TEM. The visibility of a protein lattice with square (p4) lattice symmetry confirmed the recrystallization properties of the fusion protein. So far, the biological activity of the introduced BslA moiety could not be confirmed, as rSbpA-BslA coatings did not increase the hydrophobicity on solid substrates; whether in the wet nor in the dried state (Wilhelmy plate method; contact angle measurements). It was observed, that the introduced BslA moiety favors the formation of aggregates leading to inhomogeneous coatings. The generation of alternative purification and recrystallization protocols allowing the formation of a crystalline monolayer resulting in extreme hydrophobic coatings are ongoing.

Since rheological studies, drag experiments with optical tweezers, and nanoparticle tracking analysis yielded no clear results whether the S-layer increases or decreases the flow-resistance of bacterial cells in water, or turbulences are favored or suppressed due to the nanometric topography, it was decided to enforce computer simulations of (water) flow across an S-layer protein interface. For low Reynolds numbers a fundamental solution to the Navier-Stokes equations - which describe the flow dynamics in fluids - is called Stokeslet. Stokeslets are associated with singular point forces embedded in a (creeping) Stokes flow. First results demonstrate how the velocity field is modified by the nanometer sized S-layer topography. The effect of functional groups will be introduced later.

In order to determine the diffusion constant of S-layer coated particles, dynamic light scattering (nanoparticle tracking analyses) and optical micro-rheology measurements (Zeta Sizer) were performed with S-layer coated latex beads (d= 200 nm and 1000 nm). The calculated diffusion coefficient was compared to blank and BSA coated beads. As already stated in the last report no clear conclusion could be made. So, in cooperation with IIT /Genua, Italy, a new approach using 3D particle tracking was performed. In the case of free-diffusing non-coated beads, the diffusion coefficient was calculated with 0.38 $\mu m^2/s$. For S-layer protein-coated beads, the diffusion coefficient was significantly lower having a value of 0.27 $\mu m^2/s$. The S-layer applies a dragging force to the particle, thus limiting its movement.

Finally, we continued our work related to the non-classical pathway of S-layer crystal growth on solid supports and studied the role of Fe^{2+} versus Ca^{2+} in the reassembly process. Proof-of-principle was shown that Fe^{2+} ($FeCl_2$ and $FeSO_4$) can induce the reassembly of rSbpA S-layer protein on silicon wafers. The generation of the crystalline lattice with square (p4) lattice symmetry was confirmed by AFM. A screening for suitable buffer systems, additives, $FeCl_2$ and $FeSO_4$ concentrations have been performed with the goal to stabilize iron in its Fe^{2+} state over the entire crystallization process. An important observation was the necessity that all solutions had to be prepared immediately prior to the reassembly experiments. One of the most important factors was the pH-value of the buffer solution, which had to be below 6.4. Iron might have played an important role in the reassembly process at the early stage of evolution when Fe^{2+} was most abundant.

Conclusions

The results of this project are primarily relevant for basic research but the achievements might provide the basis for novel developments in biocompatible non-wetting surfaces.

Acknowledgments

This work is funded by the Air Force Office of Scientific Research (AFOSR), Agreement award FA9550-15-1-0459.

Nut shell design and development

Nannan Xiaou[1], Peter Bock[1], Notburga Gierlinger[1]
(1) Institute for Biologically Inspired Materials, Department of Nanobiotechnology, BOKU-University of Natural Resources and Life Sciences, Muthgasse 11/II, 1190 Vienna, Austria

Aims/Objectives

Within one season some plant species produce seeds, embedded in a remarkable hard shell. Within the SCATAPNUT (Scattering and tapping on soft-hard-open nuts) project one aim is to understand how these hard nutshells are designed on the micro-and nano level, including the changes and processes from the soft to the hard tissue.

Background

One of the most important evolutionary success stories in plants is the development of seeds encased in maternal tissue, referred to as the seed coat (or testa). Some of them have a hard sustainable outer shell and are commonly known as “nuts”. By having a nutritious valuable seed they are of economic importance and research focused on the edible seed parts. Seed coats have just in the last years begun to be examined from the perspective of molecular genetics and control of development as well as for cell wall research. Furthermore recently the toughness and hardness of the outer protective layers of nuts have attracted material scientists. A hierarchical structure and the interaction of the different hierarchical levels as well as the microstructure greatly influence the macroscopic mechanical behavior and is the basis to understand structure-function relationships. A knowledge gap exists on the lower hierarchical levels: the arrangement and molecular structure of the different components making up the distinguished tissues and cells. To get access to the micro and nanostructure sample preparation approaches have to be developed. This first step is already a challenge due to the fact that nut-shells are quite hard materials when fully developed and rather soft during the first stages of development.

Results

Walnuts have been sampled from June to October and in a first step the macroscopic development of the shell is compared for three different walnut species. In June in all species only the outer green part is developed. In July the “hard” nut-shell is visible as a thin beige layer, especially in Papiernuss. In August the final nut shell is not only thicker, but also the color changes to brown. In September the nut shell seems already fully developed in thickness, but is still covered by the outer green coat. And in the final stage in October the nut shell seems homogenous, brighter and folded by shrinkage (Fig.1).

Figure 1. Photographs of different walnut species showing the development from June to October

FT-IR spectra are acquired from the different part of the nut and nut shells and afterwards details of microchemistry are revealed by Raman imaging (Fig.2.). Cryo-sections of July give excellent Raman spectra using the 532nm laser wavelength, while at the later developmental stages the rotary microtome gives better sections and autofluorescence becomes problematic. Within the beige layer of Geisenheim walnut (Fig.1, arrow) stone cells are visualized by integrating the CH-stretching (all organic cell components, Fig.2A). The cells are connected by small channels (pits), which are at this developmental stage filled with water (Fig. 2B, integrating the OH-stretching). Lignin is found in the cell wall and accumulates between the cells (Fig. 2C) already at this early stage. At the sites of high lignin accumulation also pectin can be visualized by integrating the typical marker band at 856 cm^{-1}(Fig. 2D).

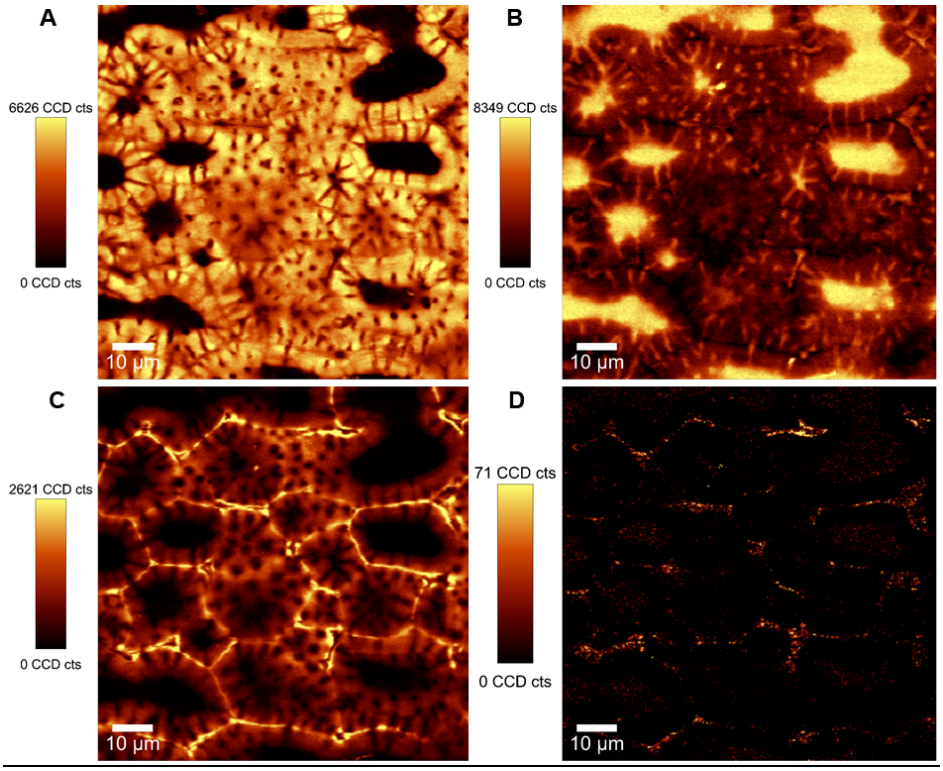

Figure 2. Microchemistry of the walnut shell at early development (Geisenheim July): A) all structures visualized by integration of CH-stretching, B) water distribution (OH-stretching), C) lignin (1600 cm^{-1}) and D) pectin (856 cm^{-1}) content.

Conclusions & Outlook

Already in the very first stages lignin accumulates especially between the stone cells, but the pit channels are still free and filled with water. Detailed analysis of these preliminary data and measurement of the other stages with different methods are underway .

Acknowledgments

This project has received funding from the European Research Council (ERC) under the European Union´s Horizon 2020 research and innovation programme (grant agreement No 681885).

Influence of a negatively charged phospholipid on the interaction of *Bacillus thuringiensis* Cyt2Aa2 toxin and lipid membrane

Itziar Otazo[1], Sudarat Tharad[1], Jose L. Toca-Herrera[1]
(1) Institute for Biologically Inspired Materials, Department of Nanobiotechnology, BOKU-University of Natural Resources and Life Sciences, Muthgasse 11/II, 1190 Vienna, Austria

Aim/Objective

A cell membrane is a lipid bilayer separating cell compartments from an environment which controls the interaction between cell and its surrounding. The lipid composition of membrane is varied among different organisms. *Bacillus thuringiensis* cytolytic toxins show their activity against a variety of cells including bacteria. Hence, Cyt toxins are possible to be a candidate for antimicrobial protein. Here, the interaction between Cyt2Aa2 and an artificial lipid membrane of bacterial cell has been studied. Since negatively charged phospholipid is found in bacterial cell, we have introduced (negative) phosphatidylglycerol (POPG) into the lipid bilayer. We have used Quartz crystal balance with dissipation (QCM-D) to monitor the deposited mass and the viscoelastic properties of the system in real time. QCM-D has also been utilized to study the influence of negatively charged lipid on the Cyt2Aa2-lipid bilayer interaction.

Results

Different conditions have been initially studied by QCM-D for lipid bilayer formation. Lipid bilayers were successfully formed in particular for a lipid composition of POPC and POPG at weight ratios 1:1 and 1:2 with presence of calcium choline ($CaCl_2$). Once the lipid bilayers were formed, two different solvents were introduced into the system: PBS and Tris-HCl buffer with $CaCl_2$. In PBS condition, Cyt2Aa2 bound on POPC/POPG membrane significantly less than on POPC/cholesterol membrane (shown in other section of this report). This is shown in Figure 1. To screen the negatively charged of POPG 10 mM of $CaCl_2$ was added to the system. Consequently, the Cyt2Aa2-lipid interaction was weaker as the decrease in frequency value and the increase in dissipation indicate (Figure 2).

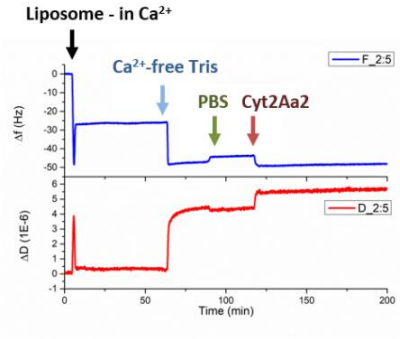

Fig.1: QCMD. POPG:POPC (1:1) Bilayer formation and protein interaction in the absence of Ca^{2+}

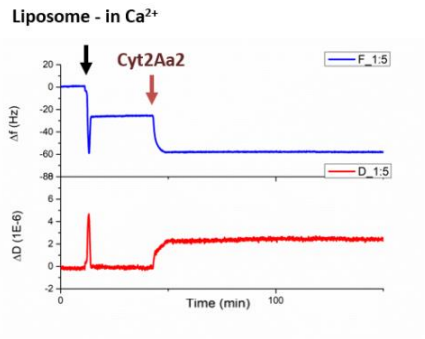

Fig.2: QCMD POPG:POPC (1:1) Bilayer formation and protein interaction in the presence of Ca^{2+}

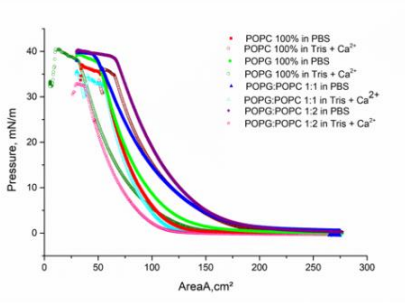

Fig.3: Langmuir-Blodgett trough monolayer characterization. Representative compression motion for both mono- (red, green) and bi-molecular (blue, purple) compositions in either PBS (closed symbols) or Tris + Ca^{2+}(open).

This result indicates that the negatively charged lipid POPG can reduce the ability of lipid binding of Cyt2Aa2. However, the Cyt2Aa2-lipid binding can take place with the presence of Ca^{2+} ion in the system. Complementarily, Langmuir trough technique was employed for the characterization of monolayer formation under the same POPC/POPG ratios as tested by QCM-D. Figure 3 shows the Langmuir isotherm of POPC/POPG lipid mixtures in PBS solution and Tris-HCl buffer with $CaCl_2$.

Conclusions

The interaction between the protein and lipid bilayer does not only depend on the lipid composition of the bilayer but also on the environmental conditions.

Acknowledgments

We would like to thank MSc. Alberto Moreno-Cencerrado and Dr. Jagoba Iturri for technical supports. This work was supported by The Austrian Science Fund (FWF) grant number: P29562-N28.

Laser induced changes of aromatics during Raman imaging of plant cell walls

Batirtze Prats-Mateu[1], Peter Bock[1], Jose L. Toca-Herrera[1], Notburga Gierlinger[1]
(1) Institute for Biophysics, Department of Nanobiotechnology, BOKU-University of Natural Resources and Life Sciences, Muthgasse 11/II, 1190 Vienna, Austria

Aim/Objective

-Determine the influence of the experimental conditions in the Raman spectra of plant cell walls, especially on the aromatic compound lignin and its monomers e.g. coniferyl alcohol
-Study the effect of repeated measurement on the aromatic structure
-Mimic the polymerization of lignin monomers in vitro by VIS laser
-Establish a calibration curve for the energy intensity (laser power and exposure time) to avoid laser induced changes in plant samples

Results

Raman images of a spruce wood microsection were taken with different excitation energy intensities (laser power and exposure time) at $\lambda ex = 532\ nm$. Concretely, concentric areas of increasing size were measured to visualize the effect in one last Raman image (Fig.1). In addition, areas of 10x10 µm^2 were repeatedly measured, up to three times, at different energy intensities. The overall intensity of the acquired Raman spectra remained constant at low energies, but decreased with the number of measurement repetition when higher energies were used, hand in hand with an increase on the background line.

The most prominent changes were observed in the bands attributed to double bond stretches (doublet at 1600 and 1660 cm^{-1}), whose ratio (1660/1600) decreased. This change was observed for low energies after the second measurement on the same area, but from the first measurement when exposure times were equal or higher than 0.1371 s and the power was higher or equal than 20 mW.

In order to study the effect of the laser energy on the aromatic polymer in Spruce wood, different stages of the aromatic lignin were used as a reference. Raman spectra were acquired in a time-series at a fixed energy intensity (1400 kJ/cm^2) for three compounds: coniferyl alcohol, a linin monomer, DHP (dehydrogenation polymer) polymerized from ferulic acid and a Spruce cell corner. For the monomer, both bands at 1600 and 1660 cm^{-1} experimented a strong exponential decay of their intensity along time. However, for DHP and cell corner the observed decay was slower, indicating that the coniferyl alcohol present in wood is the major responsible of the change in the 1660/1600 cm^{-1} ratio. Specifically, the decay rate was double in comparison to DHP.

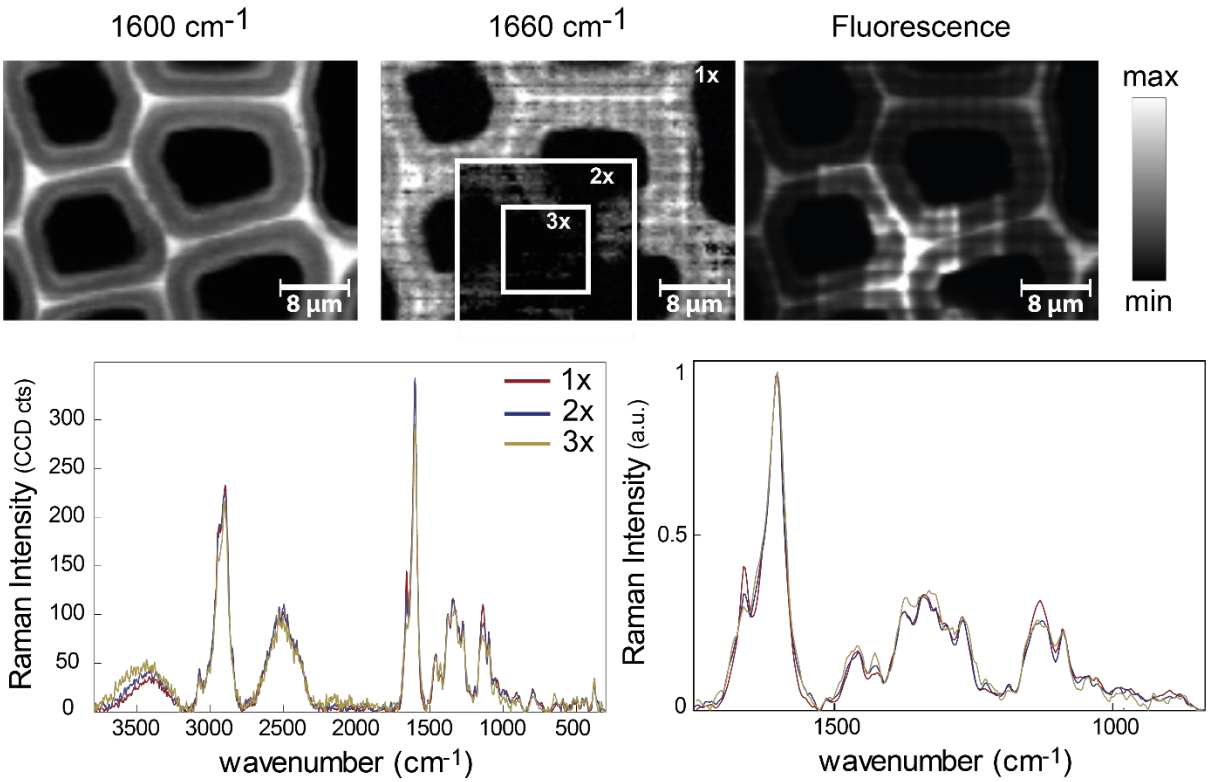

Figure 3. Raman image of Spruce microsection showing the effect of repeated laser exposure. The smallest and middle areas (3x and 2x) were exposed three and two times to the laser, respectively, which translated to a decrease of the intensity of the band at 1660 cm^{-1}. The overall intensity remained constant whereas the fluorescence (background) increased with the number of measurements.

Conclusions

The aromatic part in wood seems to be affected by the measuring conditions. This observation might be related to a further polymerization of the monomer coniferyl alcohol found in lignin.

Comparison of multivariate unmixing approaches to elucidate changes in plant cell wall chemistry and structure based on Raman images

Batirtze Prats-Mateu[1], Martin Felhofer[1], Anna de Juan[2], Notburga Gierlinger[1]
(1) Institute for Biophysics,Department of Nanobiotechnology, BOKU-University of Natural Resources and Life Sciences, Muthgasse 11/II, 1190 Vienna, Austria
(2) Chemometrics group, University of Barcelona, Diagonal 645, 08028 Barcelona, Spain

Aim/Objective

-To reveal the organization and composition of plant tissues in a non-destructive way at the micro- and nano-level with Raman imaging and multivariate data analysis.
- Ease the selection between available multivariate methods and help in the determination of analysis parameters during the analysis of Raman images of plants

Results

Three multivariate spectral unmixing algorithms, vertex component analysis (VCA), non-negative matrix factorization (NMF) and multivariate curve resolution–alternating least squares (MCR-ALS) were applied to find the purest components within datasets acquired from micro-sections of spruce wood and stem of Arabidopsis. With all three approaches different cell features, cell wall layers and cell contents were distinguished and endmember spectra with a good signal to noise ratio extracted. Even tiny layers (S1 and S3 reported to be 0.09-0.14µm thick) were elucidated based on changes in cellulose microfibril angle and subtle compositional changes. From the three unmixing methods, VCA looks as a good preliminary approach, since it is fast and does not require setting many input parameters. Spectral preprocessing (baseline correction) influenced the results obtained as well as different algorithm settings, like the different constraints applied or applying a previous principal component analysis as a filtering step. To obtain high quality spectra of the purest components or mixtures NMF or MCR-ALS are recommended.

Conclusions

Raman spectroscopic imaging combined with multivariate data analysis gives detailed insights into plant cell wall design. The Raman spectra can be used to differentiate regions different in chemistry as well as in structural organization (cellulose microfibril angle). Even subtle changes in composition and structure are visualized and based on the pure component (endmember) spectra the changes also ready to be interpreted. Nevertheless, the effect of the pre-processing approach in the analysis output has to be taken into account. The presence of the background signal can be in some cases used for the advantage of the analyst: different chemical components generate a different background and this information can be used to differentiate similar components. On the contrary, when background is present, this contribution may hinder the differentiation of subtle spectroscopic features in band signals. Therefore, the choice of baseline subtraction reveals to be very sample-dependent, and also dependent of which features want to be highlighted. When comparing all unmixing methods, main trends in components are found out consistently by all three methods, whereas differences arise in minor or very similar components. VCA is faster than the rest of the approaches and also gives good performance for

data with and without previous background subtraction. NMF works best when no background subtraction is performed. MCR-ALS showed the most different spectral signatures without using other powerful constraints for component extraction, such as local rank. It has to be taken into account that there are differences in the working procedure of the algorithms, such as a) the sequential optimization of components in VCA vs. the global optimization by NMF and MCR-ALS, b) the assumption of closure (sum of abundances equal to 1) in VCA, which is needed for the optimization, although questionable in some instances in image analysis, which is absent in NMF and MCR-ALS, 3) the PCA filtering step present in VCA and optionally in MCR-ALS, that may result in differences on the endmembers recovered. It cannot be generalized that one method gives better results than the others. It is more realistic pointing out that all the solutions provided are feasible (show similar fit and description of the variance of the original data sets). The final solutions obtained, especially for the smallest contributions, will depend on the direction of optimization that the different methods adopt and may eventually provide different interpretable aspects about the data set studied.

Acknowledgments

The authors thank the Institute of Botany at the University of Natural Resources and Life Sciences for using the rotary microtome for sectioning of the samples.

Design and characterization of pH-sensitive fluorescent probes

Damir Begic[1], Jagoba Iturri[2], Andreas Weber[2], José Luis Toca-Herrera[2]
(1) Faculty of Pharmacy, University of Sarajevo, Zmaja od Bosne 8 (Kampus), 71000 Sarajevo, Bosnia
(2) Institute for Biophysics, Dept. of NanoBiotechnology, University of Natural Resources and Life Sciences, Muthgasse 11, 1190 Wien, Austria

Aim

At the so-called chemical force microscopy the chemical modification of the tip (which can have different geometries) or even of the whole cantilever body if employing tip-less sensors, allows detecting specific and/or non-specific interactions when the tip is close enough to the sample (note that the forces involved are of molecular or colloidal range). This is also denoted as molecular recognition. If such chemical force microscopy is usually thought for specific interactions, the use of fluorescent probes might then represent an alternative to explore the chemical environment of the sample. The idea behind would be to utilize a probe which is sensitive to pH changes. Hence, knowing the variation that changes in the pH induce in the emission intensity of the fluorophore, as determined by a master curve, the fluorescent tip could act as accurate pH sensor of the substrate.

Results

Silicon dioxide and Melamine Formaldehyde (MF) particles were coated with either $(PDADMAC/PSS)_{2n/2n+1}$ or $(PEI/PSS)_{2n/2n+1}$ polyelectrolyte pairs, following a LbL deposition methodology. Along the multilayer growth, a layer consisting of negatively charged dextrane-FITC or dextrane-Rhodamine was inserted at different levels. Then, the respective fluorescent emission intensities were studied upon exposure to different buffers in the pH range between 2 and 10.

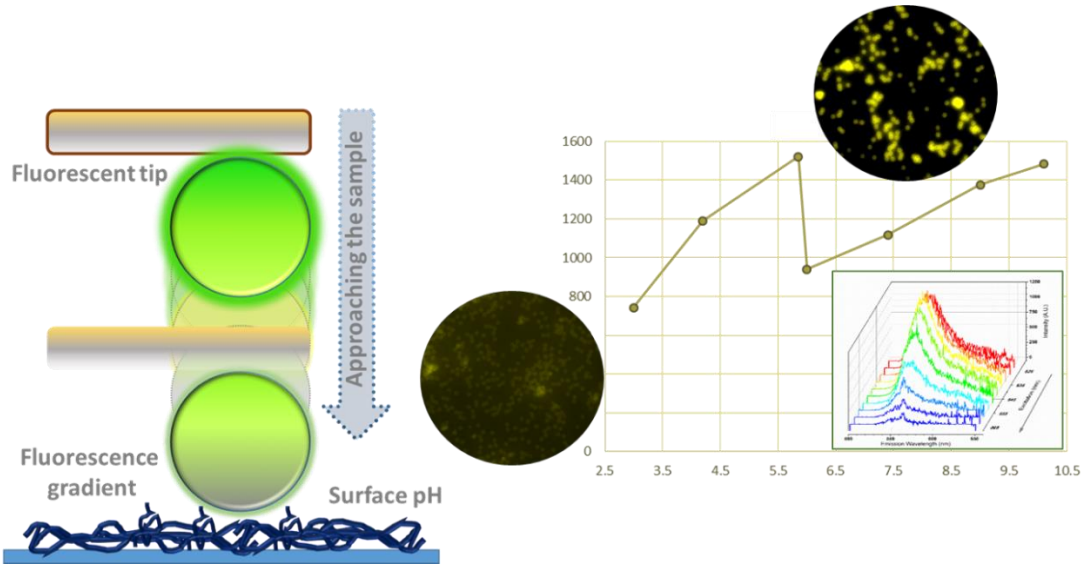

Figure 1. Left: Scheme of Fluorescence-based surface pH sensor mode, in which a stained colloidal probe is approached to the surface of interest. At sufficiently close distances the change in the pH induces quenching of the fluorescence emission. Right: Fluorescence Emission intensity variation with environmental pH for the case of FITC-cdoped LbL-coated microparticles.

Adhesion, unfolding forces, and molecular elasticity of fibronectin coatings

M. Sumarokova[1], J. Iturri[1], J. L. Toca-Herrera[1]

(1) Institute for Biophysics, Dept. of NanoBiotechnology, University of Natural Resources and Life Sciences, Muthgasse 11, 1190 Wien, Austria

Aim

The extracellular matrix fibronectin is involved in cell adhesion, growth, migration, differentiation, and wound healing. Fibronectin coatings are currently used for biomedical and biotechnology purposes. We have used force spectroscopy to study the nonspecific adhesion and unfolding properties of fibronectin coatings, as well as the unfolding (elastic) properties of fibronectin modules. We have varied both the loading rate and the residence time (Dwell time) of the AFM-tip on the fibronectin layer to evaluate the role they play in both the final adhesive and mechanical properties of the film prepared.

Results

Adhesion force between silica and fibronectin increased with loading rate delivering similar values for residence times of 1 and 2s. Further analysis indicated that the distance to the transition state was about 0.5 nm. Moreover, the adhesion force did not vary with the loading rate for contact time of 0 s. The unfolding of fibronectin domains also depended of the Dwell time (no unfolding events were observed for zero residence time). Applied loads of 2 nN were able to stretch the fibronectin layer up to 200 nm and to unfold the three fibronectin domains, which were similar for a Dwell time of 1 and 2s. However, the unfolding length increased with loading rate: below 2.5 µm s^{-1} the obtained lengths matched the value of *FN I* (13.5 nm), while for higher speeds the measured values corresponded to the lengths of *FN II* (18 nm) and *FN III* (27 nm). This investigation has answered and opened new questions about the mechanical stability and function of fibronectin coatings, mainly related to the difference between specific and nonspecific interactions that should be addressed in future works.

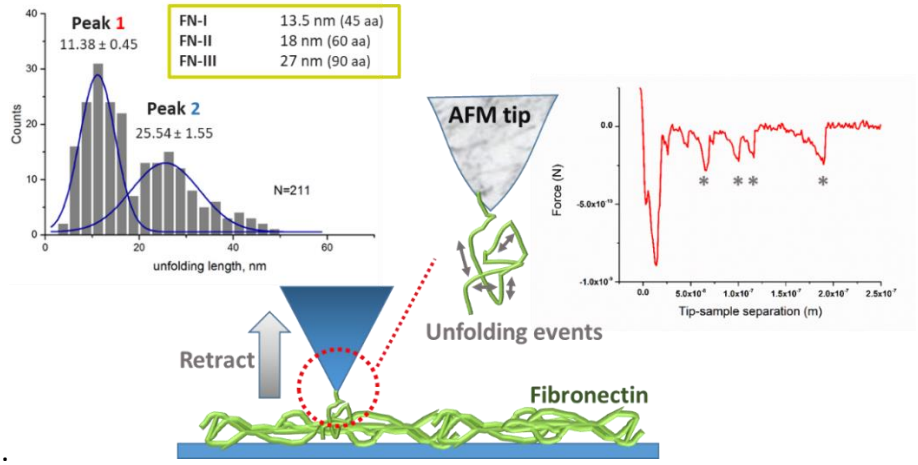

Figure1. Sketch of the Fibronectin capture and subsequent unfolding by retraction. Inset on the right shows a representative Force vs distance plot from the stretching process, where the unfolding events are highlighted by asterisks. Histogram on the left refers to the unfolding length of fibronectin at Dwell time 1 s and loading rate 1 µm s^{-1}. The number of analyzed events were N=211. The fitting shows two peaks: 11.38 ± 0.45 nm and 25.54 ± 1.65 nm. These values could correspond to the lengths of the modules FN I and FN II, respectively. The corresponding mean value for the unfolding force was 264.86 ± 10.05 pN.

Pulling rate, wettability and pH-dependent adhesion of gastric Mucin

Maria Sumarokova[1], Jagoba Iturri[1], Amsatou Andorfer-Sarr[1], Andreas Weber[1], Jose Luis Toca-Herrera[1]
(1) Institute for Biophysics, Dept. of NanoBiotechnology, University of Natural Resources and Life Sciences, Muthgasse 11, 1190 Wien, Austria

Aim

Mucus plays a crucial role in drug delivery as it is the first barrier faced by drugs or drug delivery systems prior to absorption, as it is the case of HT29 cells and Zinc ions studied in another chapter of this report. The mucus film covers and protects the body by quickly trapping foreign substances via steric and adhesive forces. In addition, many mucosa-related diseases derive from dysfunctions of the mucus barrier such as mucus hypo- or hyper-secretion and defects of its main solid component, mucins. Mucins consist of large macromolecular monomers with a protein backbone with one or more heavily glycosylated domains, rich in serine and threonine residues which serve as anchoring points for the oligosaccharide side chains (*Oh et al 2015 Eur J Pharm Biopharm*). In this work, commercially available porcine gastric mucin (CPGM) has been employed to create controlled films on glass and PEI/Chitosan substrates and their adhesive properties tested under varying conditions (environmental pH, probe wettability).

Results

A similar measuring protocol to that explained for Fibronectin films (see above) was here applied. Then, retraction of the probe took place at increasing pulling rates, and residence times of 1 and 2 s. In both cases, adhesion increased with rate and residence factors, and showing a remarkable higher binding strength for the case of the more hydrophobic probes employed (untreated Silicon Nitride).

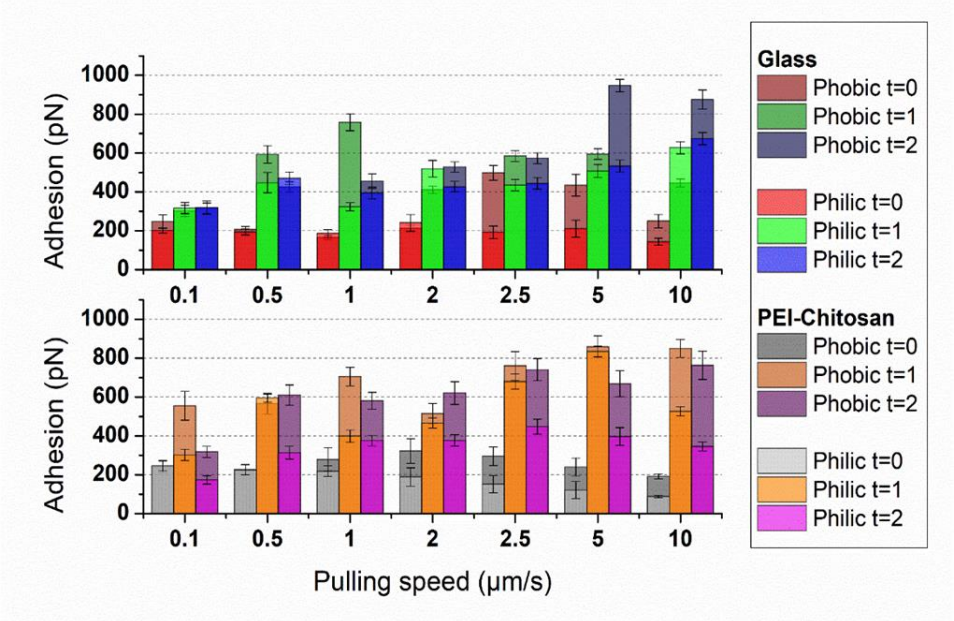

Figure 1. Maximum adhesion force calculated for Mucin films on glass or PEI/Chitosan coated slides under increasing pulling rates. Measurements regarded the use of either (hydro)philic -activated by Oxygen plasma- or (hydro)phobic tips -untreated-.

Tuning the stiffness of elastomeric surfaces to influence cell mechanics

Jagoba Iturri[1], Spela Zemljic-Jokhadar[2], Julia Miholich[1], Amsatou Andorfer-Sarr[1], Jose Luis Toca-Herrera[1]

(1) Institute for Biophysics, Dept. of NanoBiotechnology, University of Natural Resources and Life Sciences, Muthgasse 11, 1190 Wien, Austria

(2) Department of Biophysics, Medicine Faculty, University of Ljubljana, Vrazov trg 2, 1000 Ljubljana, Slovenia

Aim

Atomic Force Microscopy technique has been employed to study cell mechanics on Human Umbilical Vessel Endothelial cells (HUVEC) seeded on both elastomeric PDMS films of different stiffness, by tuning of the pre-polymer/cross-linker ratio during their preparation, and on glass (taken as reference substrate). In order to enhance the cell-substrate affinity, samples were activated by short (ca. 10 s) oxygen plasma radiation prior to cell incubation for 24 h. The variation on the mechanical properties of such films were expected to induce a different degree of cell spreading, which might have an impact on the final cell membrane mechanical response. In turn, as a result of such variation, activity of the cell upon different processes (i.e. particle absorption) might become highly influenced.

Results

Our results yielded an almost unnoticeable variation in the mechanical behavior of HUVEC cells on PDMS samples, while only the underlying presence of glass induced changes occurring. Such an observation is basically due to the hydrophilic thin silica layer created at the interface, which provides more importance to the surface wettability over substrate elasticity. When comparing the retraction segment obtained for cells on PDMS and on glass, the latter follow a clear stepwise recovery of the zero force, as a consequence of the stiffer membrane. Paxillin staining of the focal adhesions reinforced this idea by showing a homogeneous distribution of them all over the contact area, if compared to the diffuse arrangement seen for PDMS substrates.

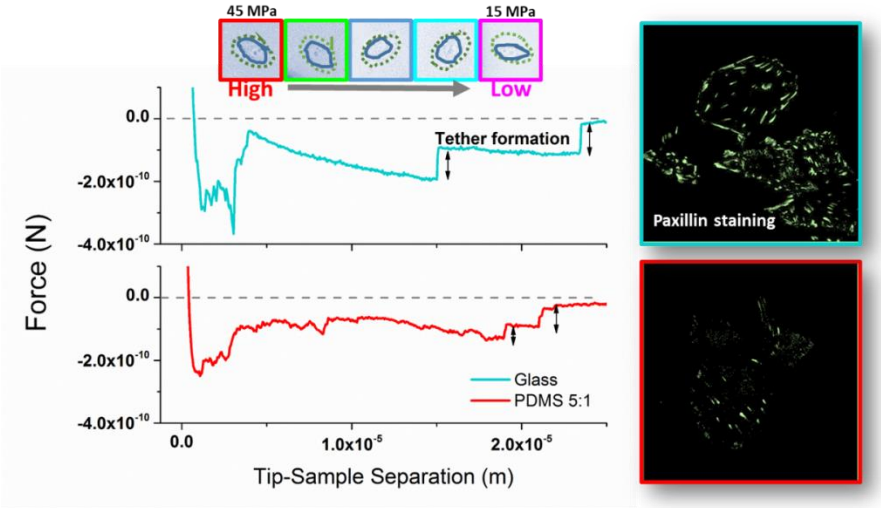

Figure 1. Left: Retraction segment showing the zero-force recovery path for HUVEC cells on either glass -light blue- or PDMS -red-. The inset on top shows the optical micrograph of HUVECs on top of varying compositions of PDMS. Right: Fluorescence microscopy images of focal adhesions formation under Paxillin staining, for HUVEC on etiher glass (top) or PDMS 5-1 (bottom).

Mechanical response of Endothelial Cells by variation of the Cytoskeleton consistency

Jagoba Iturri[1], Spela Zemlijc-Jokhadar[2], Amsatou Andorfer-Sarr[1], José Luis Toca-Herrera[1]
(1) Institute for Biophysics, Dept. of NanoBiotechnology, University of Natural Resources and Life Sciences, Muthgasse 11, 1190 Wien, Austria
(2) Department of Biophysics, Medicine Faculty, University of Ljubljana, Vrazov trg 2, 1000 Ljubljana, Slovenia

Aim

The variation of the cell mechanics on Human Umbilical Vessel Endothelial cells (HUVEC) has been studied by means of Force Spectroscopy under disturbance of the structure-supportive microfilaments within the cytoskeleton. Such alteration of the cytoskeleton could be achieved through exposure to either Cytochalasin-D (CytoD), an inhibitor of the polymerization of actin filaments, or Jasplakinolide, promoting their polymerization. Among other functions, actin filaments maintain the cell shape via extensive and intimate membrane-cytoskeleton interactions. Both interferences on the environmental conditions might induce a huge impact on the final cell membrane mechanical response.

Results

First, exposure of HUVEC cells to low concentrations of CytoD, allowed a quick and complete disruption of the internal cytoskeleton architecture, leading to a more fluid state of the whole membrane. This change was reflected by a remarkable drop in E values, and the appearance of multiple rupture events between the tip and the cell along the piezo retract -before the total loss of contact-, compared to the defined stepwise recovery (tethers) in the unaltered case. In turn, the influence of Jasplakinolide could only be detected on our preliminary results by exhaustive analysis of the pause in contact, as well as of retraction segments, with a clear impact on the rupture forces measured if compared to untreated cells.

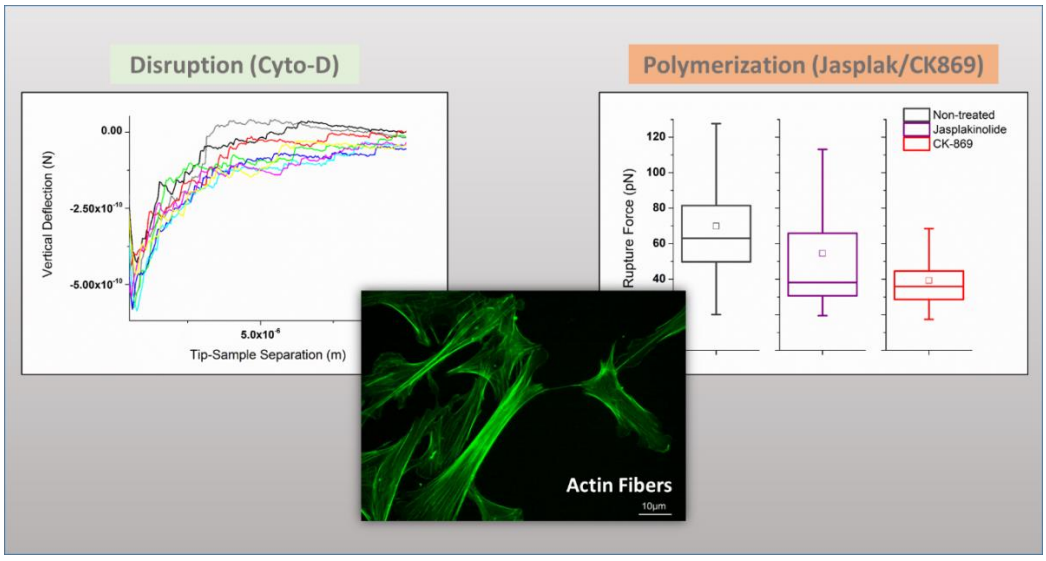

Figure 1. Impact on the mechanical response of HUVEC cells as induced by exposure to Actin-disrupting Cytochalasin-D (left) or Jasplakinolide/CK-869 factors (right) which, contrarily, favors filament polymerization.

Mechanical behavior and cell-mediated degradation of electrospun polyurethane polymer

Jagoba Iturri[1], Marjan Enayati[2], Laia Gili-Solé[1,3], Jose Luis Toca-Herrera[1].
(1) Institute for Biophysics, Dept. of NanoBiotechnology, University of Natural Resources and Life Sciences, Muthgasse 11, 1190 Wien, Austria
(2) Dept. for Biomedical research, Medicine University Wien, Spitalgasse 23, 1090 Wien, Austria
(3) University Hospital Basel, Department of Biomedicine. Hebelstrasse 20, CH - 4031 Basel, Switzerland

Aim

Polymer-based biodegradable materials have found an increasing number of medical applications in the recent years. In addition to their unique properties, these materials contribute with an on-demand adaptability which turns them into a very useful tool for the development of new devices.

In this work, complementary Electron Microscopy (SEM) and Atomic Force Microscopy techniques were employed to characterize the influence of degradation on both topographical and mechanical features of electro-spun biodegradable TPU polymer fiber-like structures, commonly used as catheters (around 60% degraded in 9 months). Samples were exposed to cultures of macrophages on top, for different periods of time, after which a cleaning of the surface takes place prior to their measurement.

Results

Films were featured by an increasing number of defects as the exposure time to macrophages was prolonged in time (see SEM picture below), together with a larger number of cellular residues. Atomic force microscopy, in turn, enabled determining the roughness and elastic modulus variation in the nano-scale for the different samples studied.

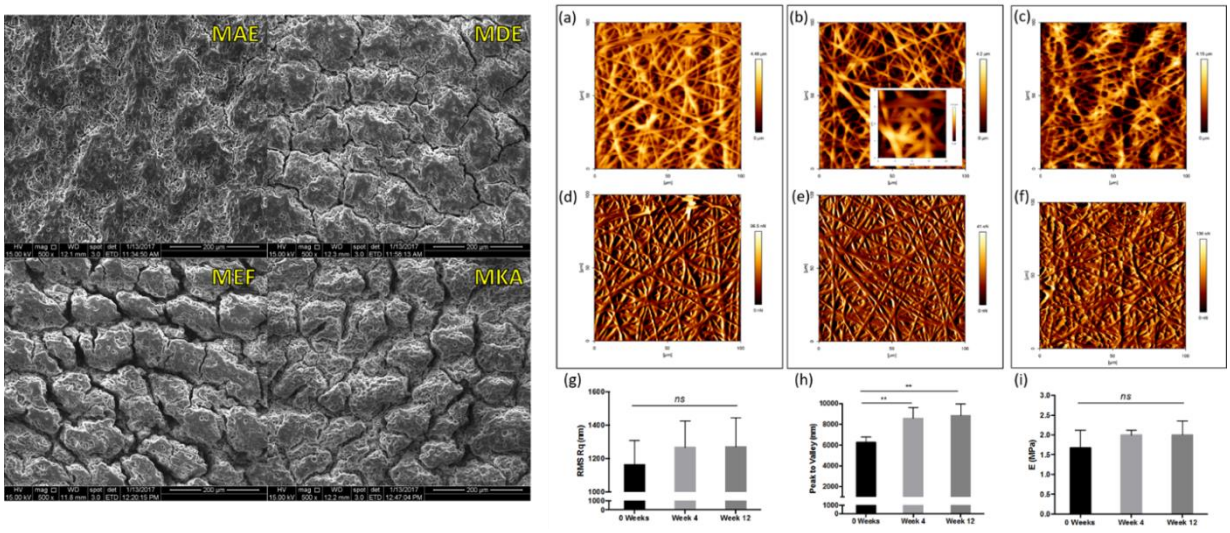

Figure 1. Left: SEM micrographs of the in-vivo samples showing the topographical degradation. Exposure time increases in the images left to right and up-down. Right: AFM microscopy height (a-c) and Vertical Deflection (d-f) images of the grafts seeded with monocyte derived macrophages at different time points. Inlet in Figure 3b highlights the presence of granular structures bound to the TPU fibers. Figures (g) & (h) show roughness and topography of the grafts identified via Rq (RMS) and peak to valley measurements. (i) Calculated Young's modulus (E) values.

Gone fishing: Using Atomic Force Microscopy for a height-dependent capture of bacterial fimbriae

Jagoba Iturri[1], Anders Lundgren[2], Peter van Oostrum[2], Erik Reimhult[2], Jose Luis Toca-Herrera[1].
(1) Institute for Biophysics, Dept. of NanoBiotechnology, University of Natural Resources and Life Sciences, Muthgasse 11, 1190 Wien, Austria
(2) Institute for Bioinspired Materials, Dept. of NanoBiotechnology, University of Natural Resources and Life Sciences, Muthgasse 11, 1190 Wien, Austria

Aim

Adhesion of bacterial cells to surfaces and the subsequent formation of a biofilm is a naturally occurring process. However, the real formation mechanism of the biofilm still represents a scientific challenge, known its relevance because of taking place on living and non-living surfaces as well as in different environments (natural, industrial and/or medical). Here, Atomic Force Microscopy (AFM) in its Force Spectroscopy mode is employed to determine the radius of action of bacterial fimbriae in the attachment to flat cantilevers under different surface modifications (specific vs non-specific).

Results

Commercially available flat AFM gold cantilevers were modified either with Mannose-thiol, inducing specific fimbriae recognition, or a molecule of hydrophobic character, such as Octanethiol. Then, the lever was positioned at different distances (in the range 0.1-2 µm) on top of the bacterial surface, and the formed interactions measured by fast retraction and analysis of the resulting adhesion peaks and unfolding events. Results showed an exponential decay in the adhesive force with increasing tip-bacteria distances for the Mannose case, while the non-specific binding yielded much weaker interactions. A trend rupturing peak observed in both systems at distances > 500 nm might indicate the thickness of a first fimbriae net after.

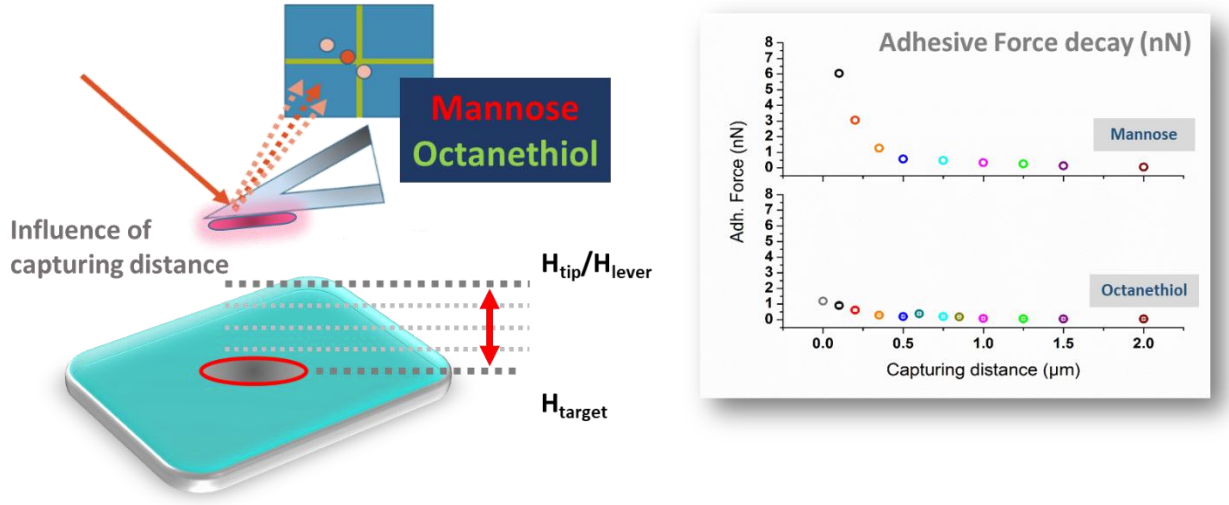

Figure 1. Left: Sketch of the measuring setup. Dashed lines indicate the different heights at which the cantilever is located. Right: Adhesive force values as obtained from the minimum in the retraction plot. It can be noted that Mannose-coated cantilevers show very high binding strengths for the shortest distances attempted (100 and 200 nm).

Role of dopamine substrates in the lineage progression of adult neural stem cells isolated from the subependymal zone.

J.M. Biscaia[1], P. Pérez-Herreras[2], Jagoba Iturri[3], Felipe Ortega[2,4,5].
(1) Faculty of biomedicine science. European University of Madrid. Calle Tajo, s/n, 28670 Villaviciosa de Odón, Madrid, Spain
(2) Biochemistry and Molecular Biology Department, Faculty of Veterinary medicine, Complutense University, Av. Puerta de Hierro s/n, 28040 Madrid, Spain
(3) Institute for Biophysics, DNBT, University of Natural Resources and Life Sciences, Muthgasse 11, 1190 Wien, Austria
(4) Institute of Neurochemistry (IUIN), Madrid, Spain.
(5) Health Research Institute of the Hospital Clínico San Carlos (IdISSC), Spain

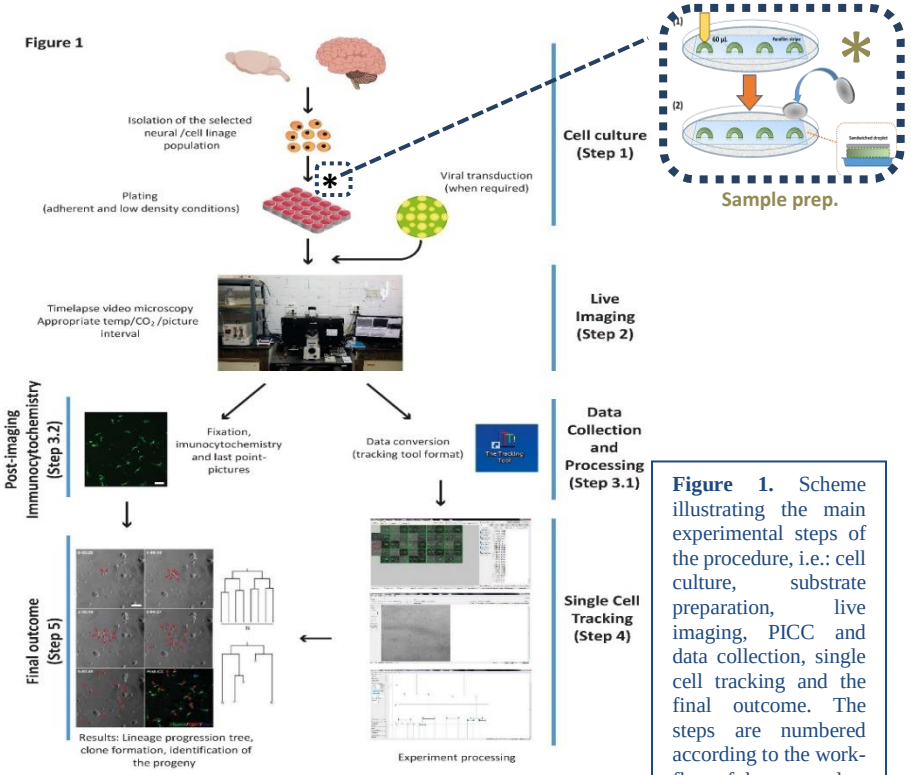

Figure 1. Scheme illustrating the main experimental steps of the procedure, i.e.: cell culture, substrate preparation, live imaging, PICC and data collection, single cell tracking and the final outcome. The steps are numbered according to the work-flow of the protocol.

<u>Aim</u>

The adult subependymal zone (SEZ) contains stem cells known as *type B* cells or adult neural stem cells (aNSCs) who give rise to fast-dividing astroglia which, in turn, generate transit-amplifying precursors (TAPs) and finally neuroblasts[1,2,3]. Because of aging the neurogenesis declines, diminishing the capacity of neuron replacement and therefore, its ability to repair damage. As a result of aging the brain displays not only a limited potential for recovery, but also, the molecular and physiological changes in the SEZ microenvironment, enhance the susceptibility to neurodegenerative diseases or injury such as stroke or demyelinating lesions[4]. Therefore, comprehending the molecular cues orchestrating the cell biology of aNSCs may lead to the design of innovative therapeutic strategies focused in the re-activation of the neurogenic niche.

In the last few years, a promising field of research placed in the activity-dependent regulation of the SEZ biology have been established, highlighting the importance of neurotransmitters in the control of the cell cycle of aNSCs[5-7]. Among them, several research groups studied the <u>role of Dopamine in the modulation of the aNSCs lineage progression</u> (transition from aNSCs to neuroblast)[8]. These studies obtained contradictory results often related to the selection of the age of the animals, the specificity of the agonists/antagonists employed or the use of the neurosphere assay that modifies the phisiologycal behavior of the aNSCs[9]. Thus, one of the best

method to study the cell biology of the aNSCs and their lineage progression still lays on live imaging. Although live imaging is currently not possible *in vivo* with the available technology, a recent method of cell culture makes the monitoring of the aNSCs lineage progression feasible *in vitro*[2, 3] (Figure 1). In this culture preparation, cells isolated from the adult SEZ are kept in absence of growth factors, with the consequence that they maintain their intrinsic neurogenic nature and allows for continuous live imaging by time-lapse video microscopy. Moreover, this culture system allowed for the first time to directly visualize asymmetric cell divisions within the lineage of aNSCs from the SEZ, thus providing a unique model for the study of NSC self-renewal.
Therefore, we combined this culture preparation with the use of dopamine and dopamine/PLL-coated glass coverslips, following the protocol by Zhang et al.[10], on which aNSCs isolated from the SEZ were seeded and their behavior analyzed by means of live imaging and single cell tracking experiments.

Results

Preliminary results suggest an interesting increase in the number of neurogenic trees as well as in the rounds of division exerted by the aNSCs (Figure 2), although new experiments are needed in order to further confirm these observations. Likewise, factors such as the potential regulation on cell cycle length, the migratory capacities and/or neuronal survival are currently under study. So far, noticeable differences were observed between control and Dopa-enriched substrates in both the neurite formation and length, pointing to a potential role of dopamine signalling in the promotion of neuronal differentiation (Figure 2). Although quite preliminary, these results are very promising and encourage us to continue in the analysis of the specific effect of the dopamine-dependent activity on the regulation of the aNSCs lineage progression.

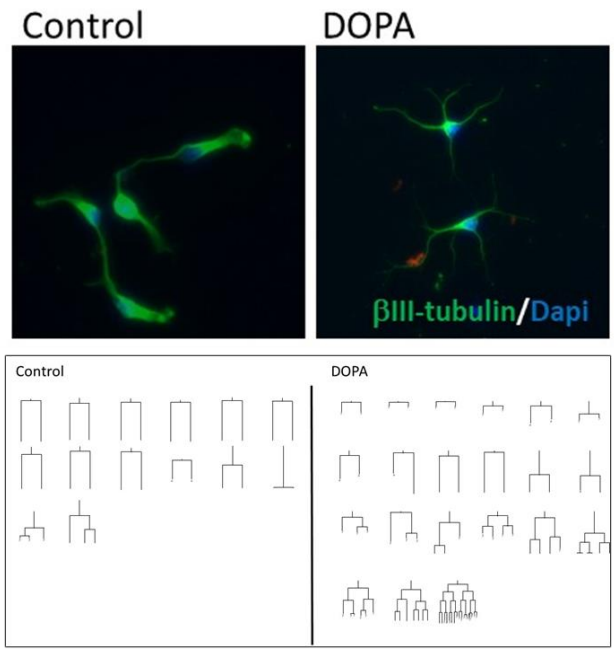

Figure 2. (Top) Neurons cultured either in PLL (Control) or DOPA substrates and labelled with the neuronal marker BIII tubulin. Note the increase in the number and length of neurites when neurons differentiated in presence of DOPA enriched substrates. (Bottom) Neurogenic lineage trees obtained after single cell tracking of one experiment of aNSCs isolated from SEZ and culture either in PLL (Control) or DOPA substrates.

References

1. Brill, M.S. et al. Nat Neurosci 12, 1524-1533 (2009). 2. Costa, M.R. et al. Development 138, 1057-1068 (2011). 3. Ortega, F. et al. Nat Protoc 6, 1847-1859 (2011). 4. Conover, J.C. et al. Aging Dis 2, 49-63 (2011). 5. Berg, D.A.et al. Development 140, 2548-2561 (2013).6. Doze, V.A. el at. Pharmacol Rev 64, 645-675 (2012). 7. Young, S.Z.et al. Front Cell Neurosci 8, 10 (2014). 8. Young, S.Z., et al. Eur J Neurosci 33, 1123-1132 (2011). 9. Pastrana, E.,et al. Cell Stem Cell 8, 486-498 (2011). 10. Zhang, Y. et al. Biomater. Sci. 3, 1188 (2015).

Controlled degradation and antifouling property loss of bacterial S-layers.

Jagoba Iturri[1], Alberto Moreno-Cencerrado[1], Jose Luis Toca-Herrera[1]
(1) Institute for Biophysics, Dept. of NanoBiotechnology, University of Natural Resources and Life Sciences, Muthgasse 11, 1190 Wien, Austria

Aim

In this work we have used SbpA S-layer protein from *Lysinibacillus sphaericus* CCM2177, in order to investigate its loss of anti-fouling activity upon controlled structural degradation. This specific protein presents a square (p4) lattice symmetry with a measured pore-to-pore distance of 13 nm (90◦ angle between adjacent protein subunits)[20]. The crystalline S-layer formation/degradation process, as well as the variation in the properties resulting from changes in the protein state, are studied by means of real time QCM-D monitoring and AFM under two distinct procedures: a) Exposure to EDTA in order to coordinate the Calcium divalent cations which are necessary to achieve the crystalline state; b) pH variations below SbpA isoelectric point (pI = 4.6), which influence the preservation of the overall crystal structure. Thus, three different scenarios are presented -and compared-in terms of antifouling efficiency: non-degraded S-layers (reference), and both EDTA- and pH-degraded S-layers. Subsequently, their respective interactions with either positively or negatively charged polyelectrolytes are studied. In addition, the three surfaces are exposed to endothelial HUVEC for cell-substrate affinity experiment purposes.

Results

Anti-fouling activity of S-layers, in addition to their structural stability in several biological environments, turns them into a potential bio-inspired coating method at the nanoscale for protecting structures and surfaces from the action of external elements. Preservation of such properties seems to be related to the degree of crystallinity of the protein layer, which involves the presence of strong protein–protein interactions resulting from optimal orientation/arrangement of the individual subunits, in combined action with divalent Ca2+ions distributed throughout the film. This cooperative activity is responsible for the strengthening and resistance of the final architecture. As shown in this manuscript, specific disturbance of these factors in the layer affects the final performance to a different extent. For instance, removal of the divalent ions by means of a chelating agent (EDTA) degrades less the crystalline structure than S-layer exposure to low pH solutions. While the former originates the appearance of structural defects and only a partial loss of the non-fouling capability, due to the remaining crystalline domains, the latter induces a total switch of the layer properties. This change is not only confirmed by the observed adsorption and spreading of HUVEC cells but also by the deposition of polyelectrolyte chains independently of their charge (positive PEI, PDADMAC vs negative PSS, BSA). The different levels of affinity obtained for the degraded S-layers might be envisaged for the design of functional coatings with an on demand degree of non-fouling efficiency.

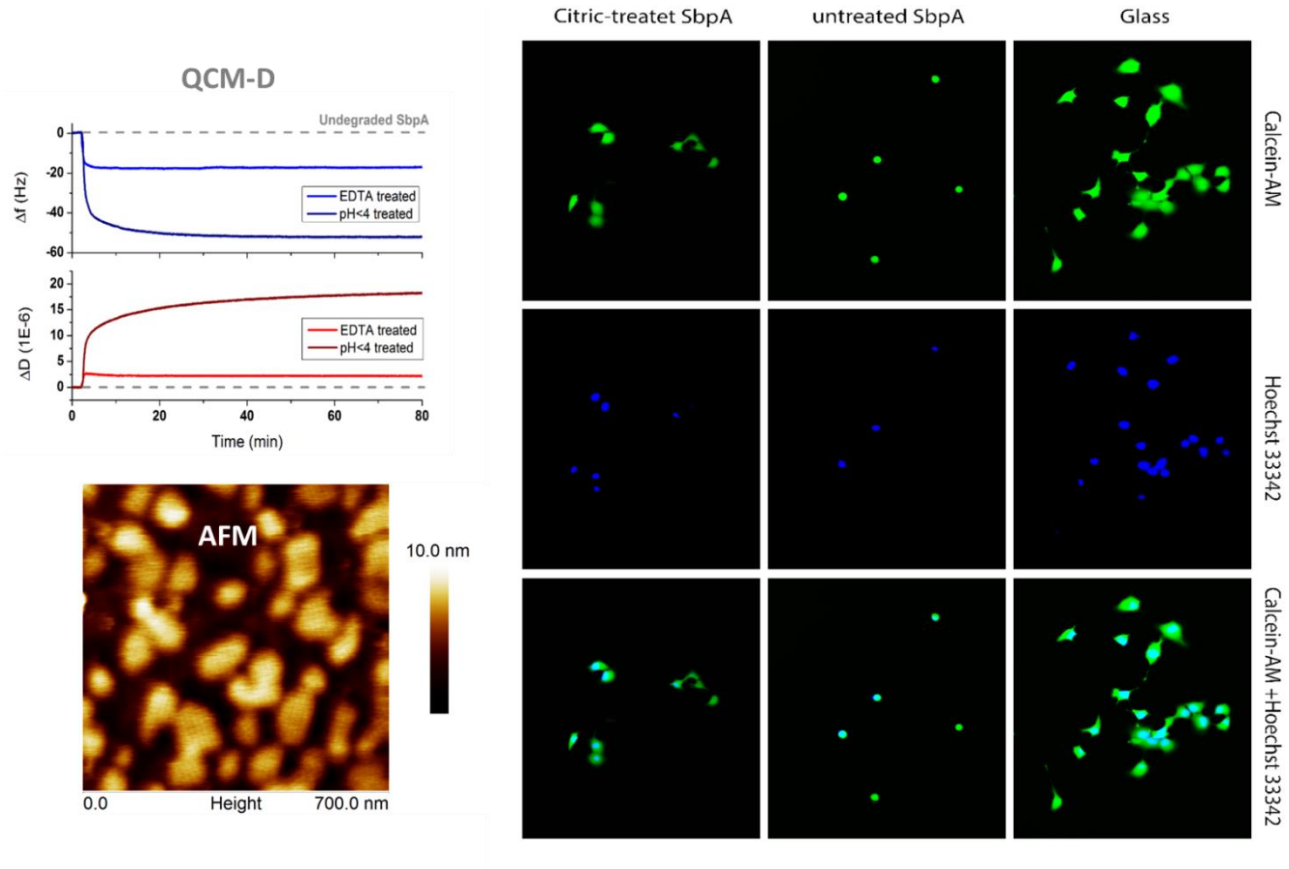

Figure 1. Left: QCMD - Δf and ΔD time variation upon exposure to HUVEC cells. The response of the degraded systems is compared to that of an untreated S-layer (dashed line). AFM - height micrographs obtained for EDTA-degraded S-layer. Right: Fluorescence Microscopy images of HUVEC cells seeded for 24 h on different substrates. Cells were stained with two different dyes: Calcein (cell membrane) and Hoescht (nuclei). The last row shows overlapping of both channels.

Voltage-induced assembly and electrical properties of S-layer films by means of combined Electrochemistry-QCMD experiments.

Jagoba Iturri[1], Andreas Breitwieser[1], Dietmar Pum[1], Uwe B. Sleytr[1], Jose Luis Toca-Herrera[1]
(1) Institute for Biophysics, Dept. of NanoBiotechnology, University of Natural Resources and Life Sciences, Muthgasse 11, 1190 Wien, Austria

Aim

The self-assembly (recrystallization) of the S-layer protein rSbpA of *Lysinibacillus sphaericus* CCM 2177 takes place i*n vitro* by the addition of Ca^{2+} ions. Kinetics, structure and properties of such coatings have been extensively detailed so far. However, in more natural environments, *L. sphaericus* bacteria could have also developed the capability of forming such 2-D coatings in the presence of other divalent ions. A controlled reproducibility of those processes in the lab is, in many cases is difficult, i.e. due tochemical instability. An example is Iron (II) ions, because of its natural tendency to oxidize to the +3 form. Therefore, protein film formation would be jeopardized under the long term incubations required to compensate kinetic limitations. To overcome such problem we used the electrochemical chamber at the QCMD. The voltage could be controlled (set to -0.1 V) from the beginning of the experiment hindering the iron to be oxidized. In addition, at the film completion one could apply electrochemical approaches (i.e. Cyclic Voltammetry) in order to study its homogeneity and electrical (insulating) performance.

Results

Recrystallization experiments of SbpA under controlled electrochemical conditions have been demonstrated to occur in the presence of $FeCl_2$ /$FeSO_4$ -instead of Ca^{2+}- in the recrystallization buffer, meaning that the recrystallization process can also be induced by Fe^{2+}. As it is crucial to maintain iron in the reduced ferrous (Fe2+) state, recrystallization buffer solutions had to be adapted accordingly (0.1M Hepes buffer pH 6.3; degased; DTT added). First supportive AFM investigations also allowed visualizing the generation of a square lattice structure.

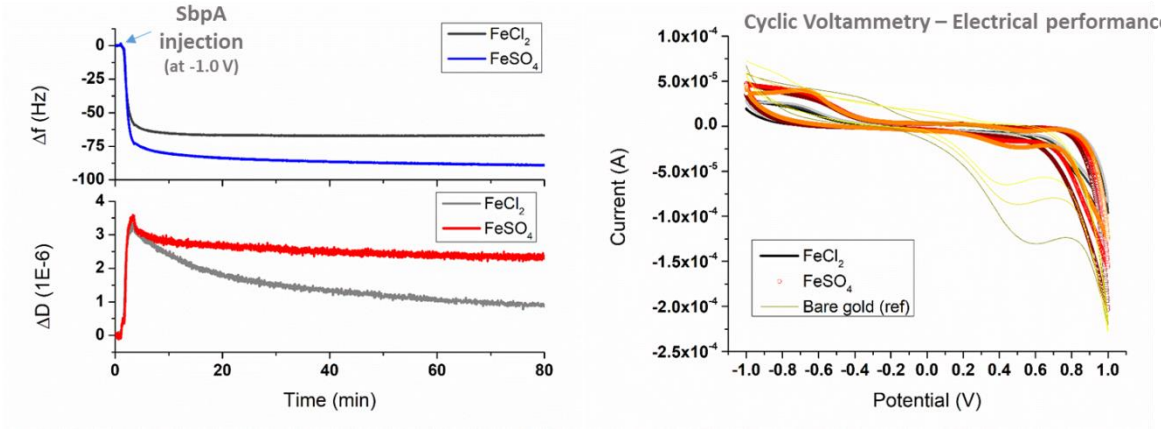

Figure 1. Left: Real time Frequency and Dissipation factors variation as monitored by QCMD for the formation of the SbpA S-layer under environmental potential control and exposure to 2 different iron (II) salts. The arrow indicates SbpA injection. Right: Cyclic Voltammogram obtained in HEPES buffer for the analysis of the preformed films and that of bare gold (as reference). Attenuation of the signal speaks about the homogeneous coating produced, being a bit more compact for $FeCl_2$ salts.

Force spectroscopy analysis on HT29-MTX mucus producing cells

J. Iturri[1], A. Moreno-Cencerrado[1], Leif Höher[2], Maria Maares[2], Claudia Keil[2], Hajo Haase[2], J.-L. Toca-Herrera[1].

(1) Institute for Biophysics, Dept. of NanoBiotechnology, University of Natural Resources and Life Sciences, Muthgasse 11, 1190 Wien, Austria

(2) Department of Food Chemistry and Toxicology, Berlin Institute of Technology, Gustav-Meyer-Allee 25, D-13355 Berlin, Germany

Aim

The mucus layer covering the intestinal epithelium has been shown to play a role in soluble ion absorption.[*G.J. Mahler et al. / Journal of Nutritional Biochemistry 20 (2009) 494–502*]. According to the mechanism proposed, Mucin proteins (present in a high percentage in mucus composition) seem to form ion-mucin complexes which enable a smoother uptake. Here, Atomic Force Microscopy together with complementary Fluorescence Microscopy is employed over mucus secreting HT29MTX (human colonic adenocarcinoma cells with resistance to methotrexate) to characterize the continuous generation of mucus affects to their mechanical response.

Results

The incubation time impact onto the mechanical properties of HT29-MTX cells was tested. Thus, cultures on top of bare (oxygen plasma treated) glass and collagen-coated glass slides were kept for 24, 48, 72 and 96 h. During the first 72 hours, cells tend to get hard, most likely because of a better attachment to the surface. Over this time, cells showed a high tissue-forming capability and the production of mucus went gradually increasing, becoming already quite significant for the maximum incubation attempted (96h).

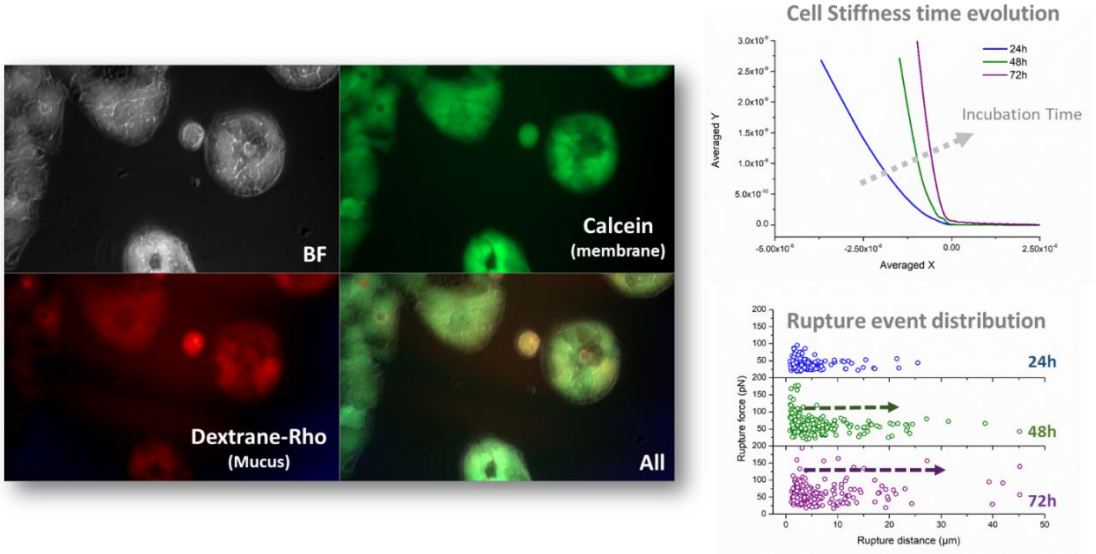

Figure 1. (left) Fluorescence and Brightfield micrographs of HT29MTX cells after 96 h of incubation. Cell membrane was stained by Calcein while Dextran-Rhodamine was employed for the mucus film. (Right, top) Representative approach segment Force-distance plots for increasing incubation times. The higher slope indicates stiffening. (Right, bottom) Distribution of the rupture events measured in the zero-force recovery path. The trend to appearing at higher positions derives from the strengthening.

Lipid membrane disruption of action of Bacillus thuringiensis cytolytic toxin Cyt2Aa2 at low protein concentration

Sudarat Tharad[1], Alberto Moreno-Cencerrado[1], Jose L. Toca-Herrera[1]
(1) Institute for Biophysics, Department of Nanobiotechnology, University of Natural Resources and Life Sciences (BOKU), Muthgasse 11, Vienna 1190, Austria

Aim/Objective

Bacillus thuringiensis Cyt2Aa2 shows a different behavior of lipid binding on a mimic lipid membrane of a mosquito cell depending on protein concentration. At high protein concentrations (≥50 μg/ml), a rigid Cyt2Aa2-lipid layer is taken place and unspecific size of lesion on the membrane is formed later. On one hand, at low protein concentration (10 μg/ml) Cyt2Aa2 aggregates on the surface of lipid membrane which is a softer layer than that of high protein concentration. As the finding above lead to the aim of this study to determine an effect of the second exposure of low protein concentration to lipid membrane. In this study, the second dose (10 μg/ml) of Cyt2Aa2 will be introduced to the system. Subsequently, the behavior of protein-lipid binding and surface topographic structure of Cyt2Aa2-lipid layer will be determined by quartz crystal balance with dissipation (QCM-D) and atomic force microscope (AFM), respectively.

Results

In our study, we found that the first exposure of Cyt2Aa2 to lipid bilayer can lead to two situations; (i) no protein binding and (ii) protein aggregate formation as observation with QCM-D and AFM. These situations are regularly taken place for the low protein concentration (10 μg/ml). Interestingly, the second exposure of Cyt2Aa2 to lipid bilayer can also induce two situations (i) growing of protein aggregates and (ii) formation of a homogenous layer with hole. QCM-D data indicate the protein-lipid interaction of the first and second at low protein concentration can lead to two different situations. Moreover, the additional information of Cyt2Aa2-lipid interaction was encouraged by AFM data which revealed the topographic surface of protein-lipid layer. In particular, time sequence of AFM height profile provided the information of the transient lesion on the membrane during protein-lipid structure rearrangement to homogenous layer. Besides, the holes in homogenous layer as well as protein aggregates were also observed after 2 hours of incubation. Nevertheless, the frequency value of QCM-D data did not indicate to any loss of material during the protein-lipid rearrangement. Our finding data indicate that the protein aggregation is the regular situation for a single exposure of Cyt2Aa2 at low protein concentration (10 μg/ml) whereas the lipid membrane disruption is possible to take place by the second dose of protein solution.

Conclusion

The combined QCM-D and AFM techniques allowed us to investigate the lipid membrane disruption of Cyt2Aa2 at low protein concentration. CytAa2 at low protein concentration is possible to disrupt the lipid membrane as the high protein concentration when the more protein is exposed to lipid membrane. Therefore, the mechanism of cytolytic toxin can be both of pore forming and detergent-like action depending on the amount of protein in the system that refer to protein concentration and the number of introduced protein.

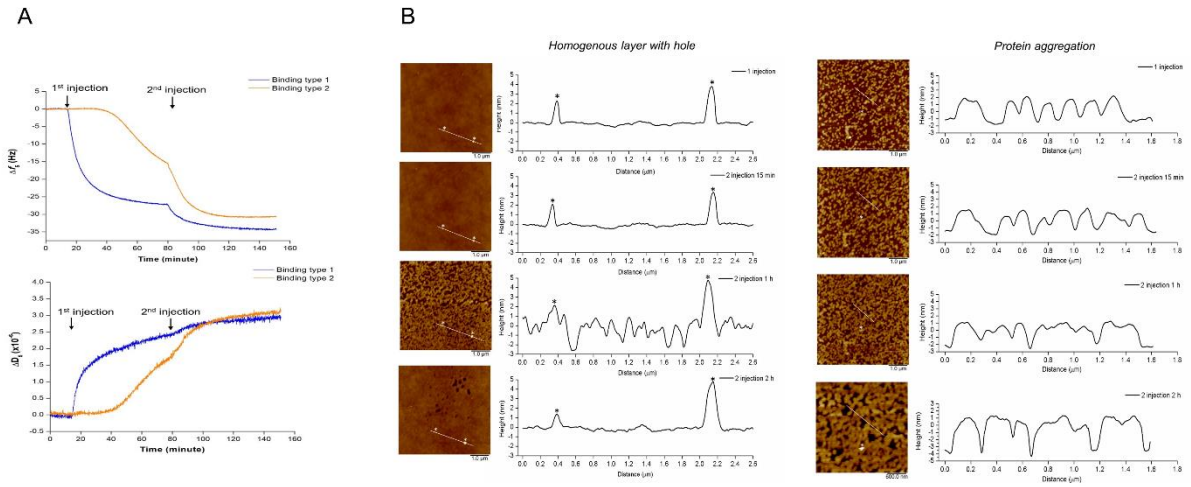

Figure 1: Cyt2Aa2-lipid bilayer interaction of low protein concentration (10 µg/ml). (A) Cyt2Aa2-lipid interaction was real-time monitored by QCM-D data at the 5th overtone. The upper panel is a frequency value plot and the lower panel is a dissipation value plot. (B) The topographic surfaces of protein-lipid layer visualized by AFM in tapping mode. The height profile of the AFM image is analyzed to determine the protein-lipid structure rearrangement in a function of time. The left panel is the homogenous layer with hole structure and the right panel is the protein aggregation structure.

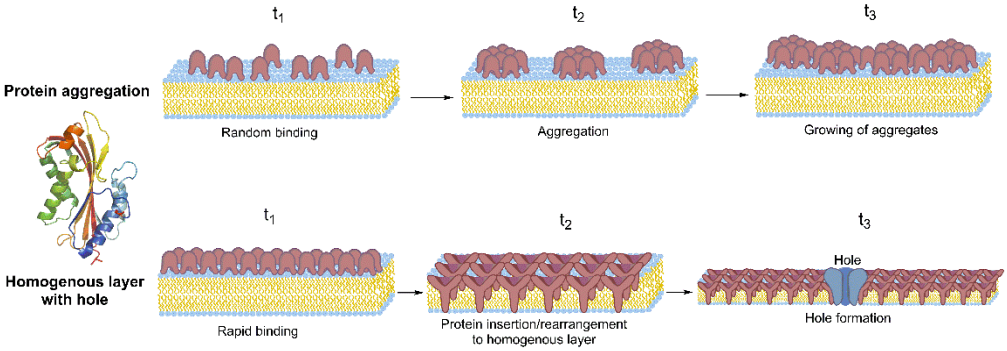

Figure 2: The model of Cyt2Aa2-lipid bilayer interaction of low protein concentration (10 µg/ml) proposed from AFM image. The second injection of low protein concentration can lead to two different protein-lipid interactions; (i) protein aggregation (upper panel) and (ii) protein-lipid homogenous layer (lower panel).

Acknowledgments

We would like to acknowledge Jacqueline Friedmann for a technical supporting. The funding of this work was supported by The Austrian Science Fund (FWF) grant number: P29562-N28.

Bacillus thuringiensis Cyt2Aa2 binding on lipid/cholesterol bilayer depends on protein concentration and time

Sudarat Tharad[1], Alberto Moreno-Cencerrado[1], Öykü Üzülmez[1], Boonhiang Promdonkoy[2], Jose L. Toca-Herrera[1]

(1) Institute for Biophysics, Department of Nanobiotechnology, University of Natural Resources and Life Sciences (BOKU), Muthgasse 11, Vienna 1190, Austria

(2) National Center for Genetic Engineering and Biotechnology (BIOTEC), National Science and Technology Development Agency (NSTDA), 113 Phahonyothin Road, Pathumthani 12120, Thailand

Aim/Objective

Bacillus thuringiensis Cyt2Aa2 toxin has a potential to use as a bioinsecticidal agent. The cytolytic mechanism of Cyt2Aa2 has been explained base on two models; pore formation and detergent-like action. However, the evidences indicating to a precise mechanism of Cyt2Aa2 are still ambiguous. Hence, the mechanism is supposed to be a protein concentration and time depended. In this study, the interaction of Cyt2Aa2 with lipid/cholesterol bilayers as a function of protein concentration and time will be determined in order to monitor protein absorption of Cyt2Aa2 at different stages. For this purpose, we combined quartz crystal microbalance with dissipation (QCM-D) with atomic force microscopy (AFM). Consequently, the protein-lipid binding kinetics will be presented concomitant with the nanostructure of protein-lipid layer.

Results

Regularly, Cyt2Aa2 protein forms holes at high protein concentration (100 μg/ml) and aggregates at low protein concentration (10 μg/ml). Moreover, those aggregates at low protein concentration (10 μg/ml) can evolve to a similar layer as the one founded at high protein concentration (100 μg/ml) with either long incubation than 3 hours or exposure of the second dose of protein solution. In this work, QCM-D results revealed that the final mass of protein-lipid layer was not significantly different. On the contrary, the rate of protein adsorption was decreased whereas the dissipation value was increased with the protein concentration decreasing. The protein adsorption process can be evaluated from the plot of dissipation value versus frequency value (D-F plot). A direction of D-F plot was distinguished for the low protein concentrations (10 μg/ml and 17.5 μg/ml) and high protein concentration (50 μg/ml and 100 μg/ml). The middle direction between them was observed for the protein concentration of 25 μg/ml. Moreover, AFM provided the protein-lipid structure during protein adsorption. In particular, a rigid hybrid layer was observed at protein concentrations of 50 μg/ml and 100 μg/ml after 30 minutes. At low concentrations, 10 μg/ml and 17.5 μg/ml, protein adsorption led to the protein aggregate on the lipid surface. Interestingly, the transition of a hole-like structure into a homogeneous layer (similar to those obtained at high concentration) was observed for a concentration of 25 μg/ml. This suggests that 25 μg/ml is a threshold concentration for the binding mechanism of Cyt2Aa2 onto lipid membranes. Concluding, the cytolytic mechanism of Cyt2A2 is possible to support by both models depending on the protein concentration and time of incubation used in the experiment.

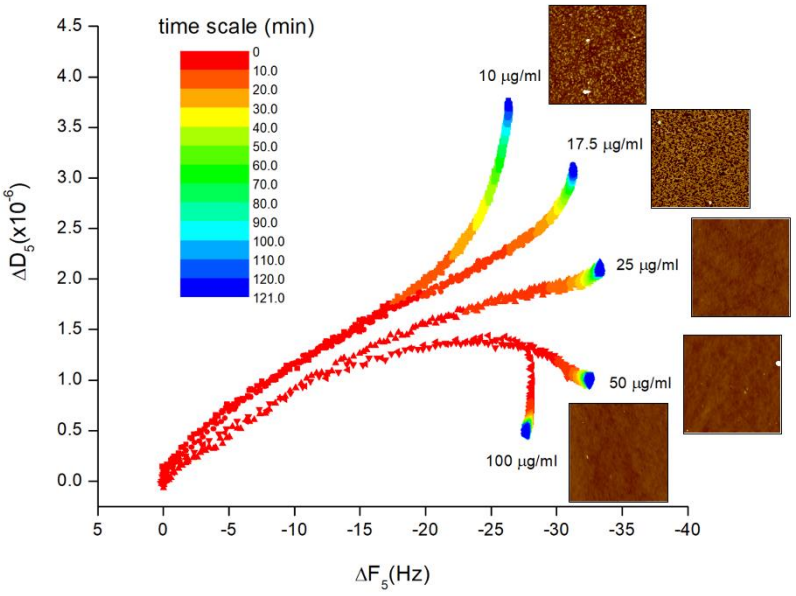

Figure 1: The D-F plot of Cyt2Aa2-lipid interaction at various protein concentrations presenting the distinct adsorption process of Cyt2Aa2. AFM topographic image of the final protein-lipid layer (at 2 hours of incubation) is presented at the end of plot.

Acknowledgments

This work was supported by The Austrian Science Fund (FWF) grant number: P29562-N28.

Effect of cholesterol on *Bacillus thuringiensis* Cyt2Aa2 binding on the lipid membrane

Sudarat Tharad[1], Öykü Üzülmez[1], Boonhiang Promdonkoy[2], Jose L. Toca-Herrera[1]

(1) Institute for Biophysics, Department of Nanobiotechnology, University of Natural Resources and Life Sciences (BOKU), Muthgasse 11, Vienna 1190, Austria
(2) National Center for Genetic Engineering and Biotechnology (BIOTEC), National Science and Technology Development Agency (NSTDA), 113 Phahonyothin Road, Pathumthani 12120, Thailand

Aim/Objective

Bacillus thuringiensis cytolytic toxins (Cyt toxin) show their activity against a variety of cell type e.g. insect cells and mammalian cells. A factor which play an important role for Cyt2Aa2 activity including an amino acid residue and lipid composition of membrane have been studied for a few decades. As reported in the literature, the unsaturated phospholipid is required for cytolytic activity while cholesterol does not show any effect. However, a level of cytolytic activity of Cyt2Aa2 is different among an organism. Their lipid membranes contain a different lipid composition including the amount of cholesterol. In this work, a level of cholesterol in lipid membranes will be varied to determine an effect on the lipid binding behavior of Cyt2Aa2. To reach this objective, quartz crystal microbalance with dissipation (QCM-D) will be carried out to determine a deposited mass and viscosity of protein-lipid layer.

Results

Lipid bilayers were formed containing different amounts of cholesterol. The mixture lipid of 1- palmitoyl-2-oleoyl-sn-glycero-3-phosphocholine (POPC) and cholesterol was varied to ratio; 5:0.2, 5:1, 5:2 and 5:3 by weight. The changes of cholesterol level in lipid membrane affect to (i) a hydrodynamic radius of liposome and (ii) a thickness of lipid bilayer. The value of them trend to increase with a higher level of cholesterol in lipid membrane. The changes of frequency and dissipation values of lipid bilayer were not significantly different with QCM-D study. Although, a distinction of protein-lipid binding behavior of Cyt2Aa2 was observed when the cholesterol level was raised to ratio of 5:3 (POPC:cholesterol by weight). The frequency and dissipation values of Cyt2Aa2 binding were approximately higher than the other lipid composition for 8-fold and 18-fold, respectively. Moreover, the cholesterol level was also affected on the protein-lipid binding of Cyt2Aa2 mutant. Threonine residue-144 (T144) has been proposed to involve in lipid binding of Cyt2Aa2. Mutation of T144 to Alanine (T144A) results in a reduction of a hemolytic activity of Cyt2Aa2 about 2-folds. T144A mutant bound on POPC/cholesterol membrane with the lipid ratio of 5:3 whereas no binding was observed for the lipid ratio of 5:0.2. Interestingly, the ability of lipid binding of T144A mutant was less than Cyt2Aa2 wild type as correspond to the hemolytic activity. These results reveal a novel effect of cholesterol on protein-lipid binding of Cyt2Aa2, not only alter the lipid binding behavior of Cyt2Aa2 wild type but encourage lipid binding of T144A mutant also.

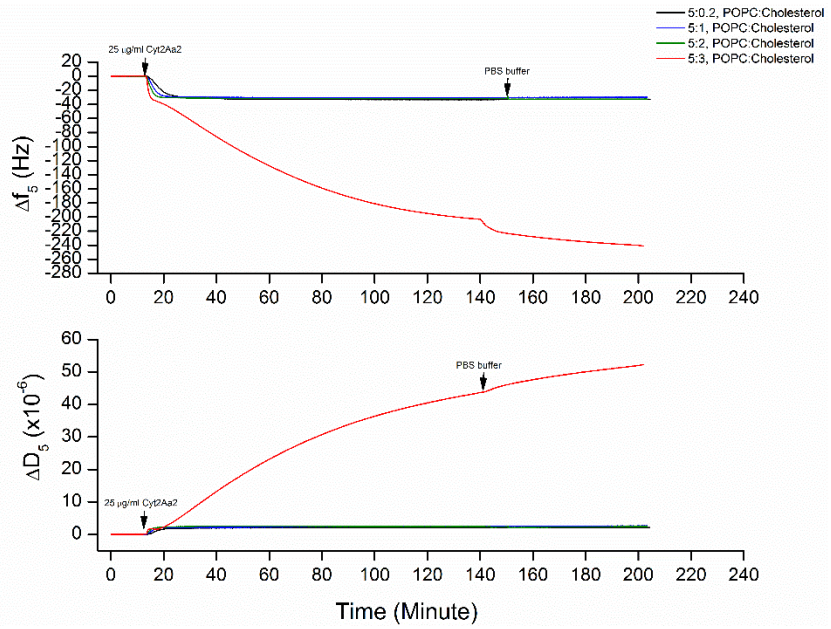

Figure 1: Cyt2Aa2 wild type interaction with POPC/cholesterol membrane containing a different level of cholesterol. Frequency and dissipation values are presented at the 5th overtone.

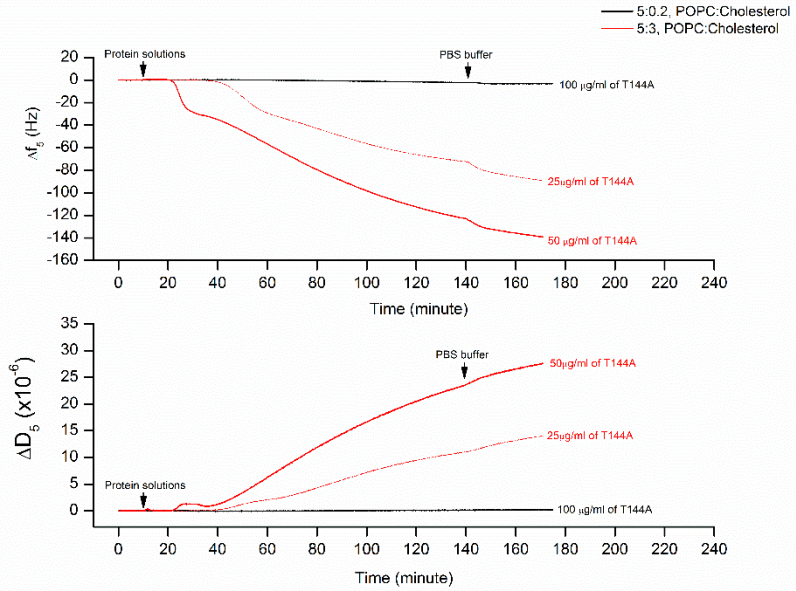

Figure 2: Cyt2Aa2 T144A mutant interaction with POPC/cholesterol membrane containing a different level of cholesterol. Frequency and dissipation values are presented at the 5th overtone.

Acknowledgments

This work was supported by The Austrian Science Fund (FWF) grant number: P29562-N28.

In-situ 2D bacterial crystal growth as a function of protein concentration

Alberto Moreno-Cencerrado[1], Jagoba Iturri[1], Violetta Gołębiewska[1], José L. Toca-Herrera[1]
(1) Institut für Biophysik, DNBT, BOKU University for Natural Resources and Life Sciences, Vienna, Austria.

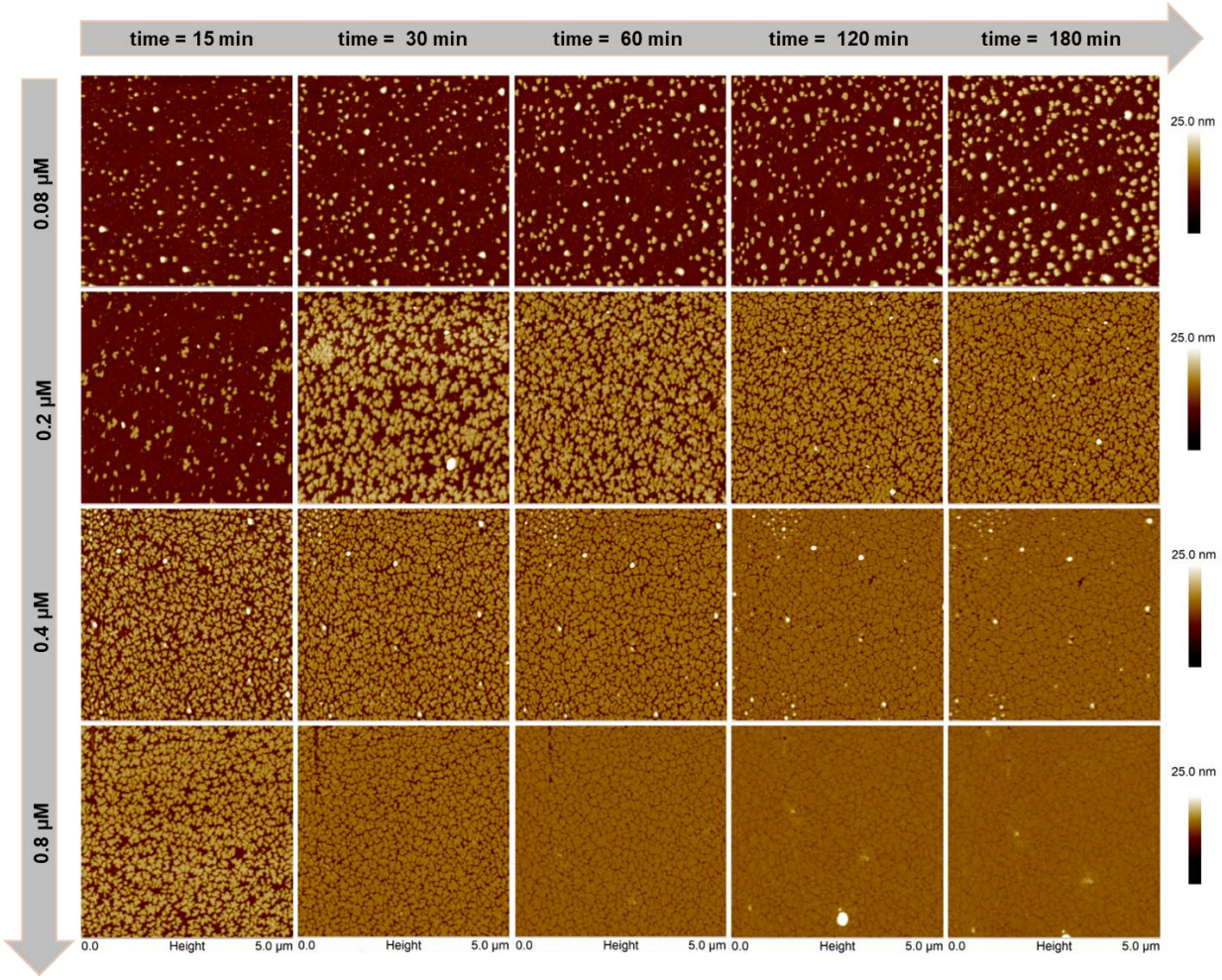

Figure 1. Interplay of the time with the protein concentration for all the cases presented in this study. A clear increment of the film formation capability can be observed from top-left to bottom-right micrographs, as both the SbpA concentration and observation time increase.

Aim/Objective

In this work, we have investigated the adsorption and crystal growth of SbpA proteins at hydrophobic fluoride-functionalized SiO2 surfaces as a function of the interplay between protein concentration and (observation) time. The experimental results have been modeled with the classical adsorption and crystal growth models. These experiments provided new insight into the understanding of protein adsorption and 2D protein crystallization.

Results

The interplay between protein concentration and (observation) time has been investigated for the adsorption and crystal growth of SbpA proteins on hydrophobic fluoride-functionalized SiO2 surfaces. The amount of the adsorbed mass protein and the viscoelastic properties of the formed protein layer have been studied with Quartz Crystal Microbalance with Dissipation (QCM-D). Crystal growth and the corresponding lattice parameters have been resolved by Atomic Force Microscopy (AFM). Both techniques show: 1) that crystal formation occurs only

by exposure to concentrations above a threshold value (0.08 μM) and after a certain degree of coverage (ca. 70% of the initial protein), and 2) the compliance of the formed crystal decreases for increasing protein concentration. All the crystal domains observed presented similar lattice parameters (e.g. a = 13.6 ± 0.2 nm, b = 13.6 ± 0.2 nm, γ = 89° ± 2). Protein film formation is shown to take place from initial nucleation points which originate a gradual and fast extension of the crystalline domains. The application of the theoretical models (Langmuir and Avrami) suggest that protein-surface interactions prevail over protein-protein interactions.

Conclusions

The combination of QCM-D and AFM represents a robust method to study protein adsorption and two-dimensional protein crystal growth. In the case of SbpA, two conditions for crystal formation were observed: 1) to expose the host substrate to a concentration equal or larger than 0.08 μM, and 2) a minimum number of nucleation points, which appear once the 70% of the total adsorbed mass is achieved.

According to the analysis of the results, protein-surface interactions dominate over protein-protein interactions in SbpA crystal formation. Although the lattice parameters remain invariant, the compliance of the final crystal depends on the initial protein concentration. This fact is directly related to the confluence and the boundary defects of the crystal domains.

An open question is if larger experimental times would contribute to the confluence of the crystal at lower protein concentrations (above 0.08 μM). This work shows that QCM-D, AFM and digital imaging processes can provide new insights on molecular self-assembly and crystal growth. Furthermore, the results obtained with such techniques can be used to test or develop theoretical models and theories.

Acknowledgments

Part of this work was supported by the International Graduate School BioNanoTech (IGS) Program of the Federal Ministry for Science and Research, Austria, and the Air Force Office of Scientific Research (AFOSR) (Grant FA9550-12-1-0274). Authors acknowledge Dietmar Pum, and Uwe Sleytr for exciting discussions, and also Jacqueline Friedmann for technical support.

State of the Art of the interaction between cytolytic proteins and lipid-cholesterol bilayers

A. Moreno-Cencerrado[1], S. Tharad[1], T. Bogataj[1], J. Iturri[1], B. Promdonkoy[2], C. Krittanai[2], J.L. Toca-Herrera[1]

(1) Institute for Biophysics, Department for NanoBiotechnology, University of Natural Resources and Life Sciences, Muthgasse 11, 1190 Vienna Austria

(2) Institute of Molecular Biosciences, Mahidol University, 25/25 Phuttamonthon 4 Road, Salaya Campus, Nakhon Pathom 73170, Thailand

Aim/Objective

Bacillus thuringiensis Cyt2Aa2 proteins show toxicity against insect larvae and some eukaryotic cells. Lipid-cholesterol bilayer models are a suitable tool to investigate their toxicity mechanism at molecular scale in the laboratory. In this work, we show how toxin concentration and observation time influence the lipid-protein interaction and the final nanostructure of the hybrid lipid-protein layer. Quartz Crystal Microbalance with Dissipation (QCM-D), Atomic Force Microscopy (AFM), and Langmuir–Blodgett trough (LBT) have been used to analyze such phenomena.

Results

Quartz Crystal Microbalance with Dissipation (QCM-D) and Atomic Force Microscopy (AFM) studies revealed that the exposition of the lipid-cholesterol bilayer to 0.30 µM protein concentration during two hours led to the formation of aggregates (detergent-like mechanism). On the contrary, a rigid homogeneous lipid-protein layer was formed when the lipid system interacts with 3.00 µM of toxins (pore-forming model mechanism).

However, on one hand, QCM-D results indicated that at the lowest protein concentrations the hybrid system may not be at equilibrium. New AFM investigations confirmed that those aggregates disappear forming a hybrid homogeneous layer similar to the case of the highest concentration (but more liquid-like). On the other hand, QCM-D results suggest that the addition of new proteins after seventy minutes led to a new type of lipid-protein layer. Finally, AFM studies showed that a second addition of protein to the lipid-cholesterol bilayer induced face separation in a time frame of minutes, as it is illustrated in the Figure.

Complementary studies concerning the interaction of lipid-cholesterol monolayers and the toxin were carried out with Langmuir-Blodgett films. Preliminary results confirmed the importance of the lipid/cholesterol ratio and the phospholipid chain length on the monolayer stability against the effect of cytolytic proteins (monolayer rupture).

Acknowledgments

Authors would like to thank Iris Strube (Biophysics Institute, DNBT – BOKU) for technical support. This work was supported by the Thailand Research Fund (TRF) through the Royal Golden Jubilee Ph.D. Program (RGJ) (Grant No. PHD/0116/2551), the National Center for Genetic Engineering and Biotechnology (BIOTEC), National Science and Technology Development Agency, Thailand (NSTDA), and the International Graduate School BioNanoTech (IGS) Program of the Federal Ministry for Science and Research (Austria).

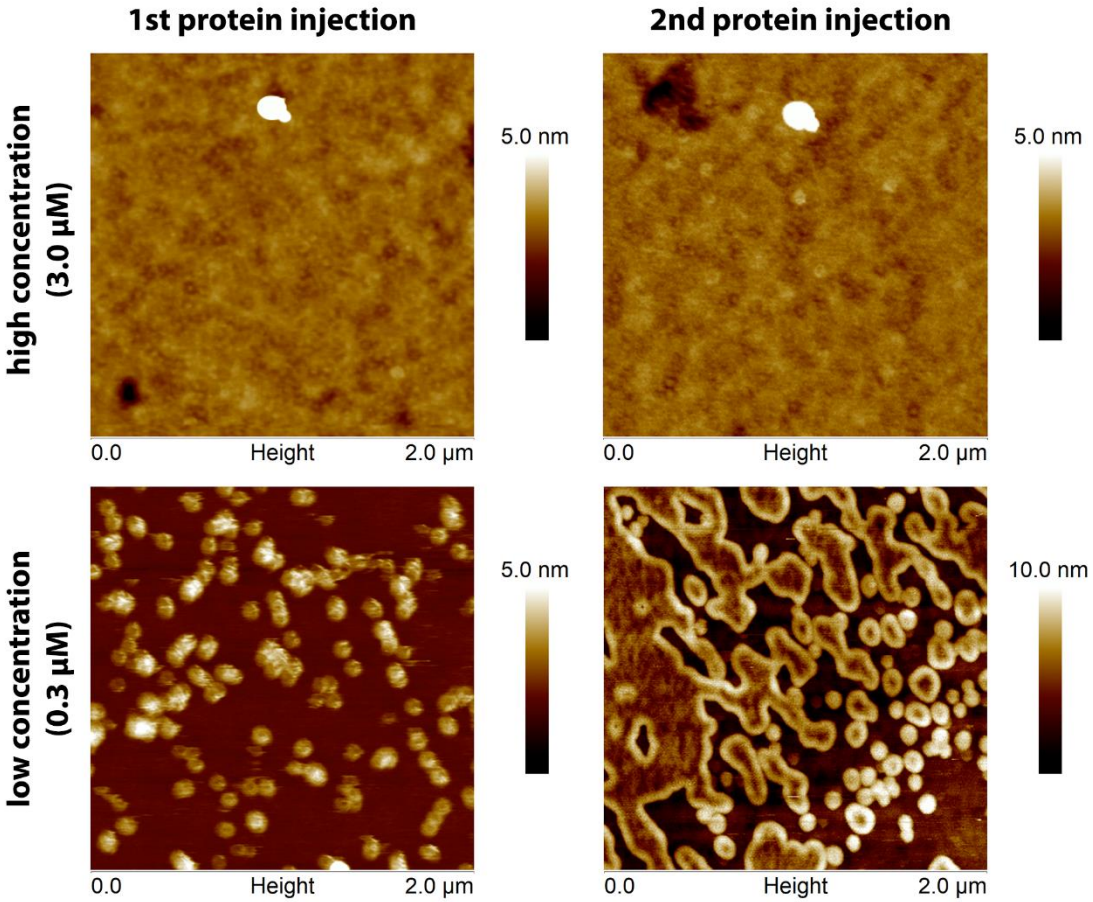

Figure 1: Topography of the four cases under analysis. In the upper row, the Cyt2Aa2 proteins form a confluent layer with the presence of some hole-like defects after two hours. A second injection of proteins into the chamber does not significantly change the hybrid layer. In the lower row, Cyt2Aa2 proteins at low concentration after 2h form rounded island-like structures. Then, a second injection of proteins induces a drastic change in the hybrid protein-lipid/cholesterol layer.

Analyzing Spatial Behavior of Backcountry Skiers in Mountain Protected Areas Combining GPS Tracking and Graph Theory

Karolina Taczanowska[1], Mikołaj Bielański[2], Luis-Millán González[3], Xavier Garcia-Massó[4], José L. Toca-Herrera[5]

(1) Institute of Landscape Development, Recreation and Conservation Planning, Department of Landscape, Spatial and Infrastructure Sciences, University of Natural Resources and Life Sciences (BOKU), 1180 Vienna, Austria

(2) Department of Tourism and Recreation, University School of Physical Education, 31-571 Cracow, Poland

(3) Department of Physical Education and Sport, University of Valencia, 46010 Valencia, Spain

(4) Departament de Didàctica de l'Expressió Musical, Plàstica i Corporal, University of Valencia, 46010 Valencia, Spain

(5) Institute for Biophysics, Department of Nanobiotecnology, University of Natural Resources and Life Sciences (BOKU), 1190 Vienna, Austria

Aim/Objective

Mountain protected areas aim to preserve vulnerable environments encouraging simultaneously their use for leisure activities.

Our study aims to develop an approach to evaluate the structure and use of designated skiing zones in PAs combining Global Positioning System (GPS) tracking and analytical methods based on graph theory.

Results

The study was based on empirical data (n = 609 GPS tracks of backcountry skiers) collected in Tatra National Park (TNP), Poland. First, the physical structure of the entire skiing zones system was simplified into a graph structure (structural network; undirected graph). In a second step, the actual use of the area by skiers (functional network; directed graph) was analyzed using a graph-theoretic approach. Network coherence (connectivity indices: β, γ, α), movement directions at path segments, and relative importance of network nodes (node centrality measures: degree, betweenness, closeness, and proximity prestige) were calculated. The results show that the system of designated backcountry skiing zones was not evenly used by the visitors. Therefore, the calculated parameters differ significantly between the structural and the functional network. In particular, measures related to the actually used trails are of high importance from the management point of view. Information about the most important node locations can be used for planning sign-posts, on-site maps, interpretative boards, or other tourist infrastructure.

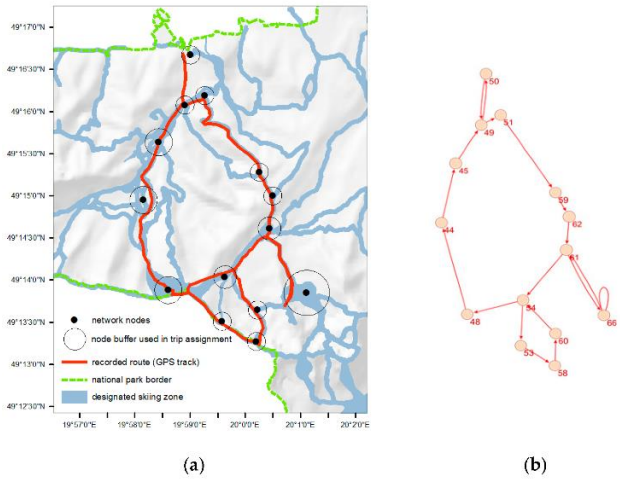

Figure 1: Skiing route. (a) Recorded GPS track of a TNP visitor. (b) Corresponding directed graph G = (V,E) where the vertices are V = {44,…,66} and the edges are E = {(50, 49), (49, 51), (51, 59), (59,62), (62, 61), (61, 66), (66, 61), (61,54), (54, 53), (53, 58), (58, 60), (60, 54), (54, 48), (48, 44), (44, 45), (45, 49), (49, 50)}. In the final graph the loop, (66, 66) was deleted, since a property of directed graphs is vi ≠ vj.

Acknowledgments

Univ. Valencia (UV-INV EPDI15-276152). ÖEAD (S&T Cooperation/WTZ grant number PL01/2016). Tatra National Park and Dept. Tourism & Recreation (Cracow).

2. Articles, book chapters, conferences, seminars, workshops and schools

Publications (SCI articles)

Breitwieser A, Iturri, J, Toca-Herrera JL, Sleytr UB, Pum, D
In Vitro Characterization of the Two-Stage Non-Classical Reassembly Pathway of S-Layers
Int J Mol Sci 18 (2017) 400, DOI: 10.3390/ijms18020400

De Meester B, de Vries L, Özparpucu M, Gierlinger N, Corneillie S, Pallidis A, Goeminne G, Morreel K, De Bruyne M, De Rycke RM, Vanholme R, Boerjan WA
Vessel-specific reintroduction of CINNAMOYL COA REDUCTASE 1 (CCR1) in dwarfed ccr1 mutants restores vessel and xylary fiber integrity and increases biomass
Plant Physiol. (2017), DOI: 10.1104/pp.17.01462

Gierlinger N
New insights into plant cell walls by vibrational microspectroscopy
Applied Spectroscopy Reviews (2017) 1-35, DOI: 10.1080/05704928.2017.1363052

Huss JC, Schoeppler V, Merrit DJ, Best Ch, Maire E, Adrien J, Spaeker O, Janssen N, Gladisch J, Gierlinger N, Miller BP, Fratzl P, Eder M
Climate-Dependent Heat-triggered Opening Mechanism of Banksia Seed Pods
Advanced Science 5 (2017) 1700572, DOI: 10.1002/advs.201700572

Iturri J, Moreno-Cencerrado A, Toca-Herrera, JL
Polyelectrolyte brushes as supportive substrate for bacterial S-layer recrystallization: Polymer charge and chain extension factors
Colloids Surf A 526 (2017) 56, DOI: 10.1016/j.colsurfa.2016.10.070

Iturri J, Moreno-Cencerrado A, Toca-Herrera JL
Cation-chelation and pH induced controlled switching of the non-fouling properties of bacterial crystalline films
Colloids Surf B. 158 (2017) 270, DOI: 10.1016/j.colsurfb.2017.07.003

Iturri J, Toca-Herrera JL
Characterization of Cell Scaffolds by Atomic Force Microscopy
Polymers 9 (2017) 383, DOI: 10.3390/polym9080383

Iturri J, Vianna AC, Moreno-Cencerrado A, Pum D, Sleytr UB, Toca-Herrera JL
Impact of surface wettability on S-layer recrystallization: a real-time characterization by QCM-D
Beilstein J Nanotechn 8 (2017) 91, DOI:10.3762/bjnano.8.10

Moreno-Cencerrado A, Iturri J, Pecorari I, Vivanco MdM, Sbaizero O, Toca-Herrera JL
Investigating cell-substrate and cell-cell interactions by means of single-cell-probe force spectroscopy
Microsc Res Tech 80 (2017) 124, DOI: 10.1002/jemt.22706

Kuprian E, Munkler C, Resnyak A, Zimmermann S, Tuong TD, Gierlinger N, Müller T, Livingston DP, Neuner G
Complex bud architecture and cell-specific chemical patterns enable supercooling of Picea abies bud primordia
Plant Cell Environ. 40 (2017) 3101, DOI: 10.1111/pce.13078

Ozparpucu M, Ruggeberg M, Gierlinger N, Cesarino I, Vanholme R, Boerjan W, Burgert I Unravelling the impact of lignin on cell wall mechanics: a comprehensive study on young poplar trees downregulated for CINNAMYL ALCOHOL DEHYDROGENASE (CAD)
Plant Journal 91 (2017) 480, DOI: 10.1111/tpj.13584

Prats-Mateu B, Harreither, E, Schosserer M, Puxbaum V, Gludovacz E, Borth N, Gierlinger N, Grillari J Label-free live cell imaging by confocal Raman microscopy identifies CHO host and producer cell lines
Biotechnol J 12 (2017) 1, DOI: 10.1002/biot.201600037

Prats-Mateu B, Gierlinger N
Tip in–light on: Advantages, challenges, and applications of combining AFM and Raman microscopy on biological samples
Microsc Res Techn 80(2017) 30, DOI 10.1002/jemt.22744

Tharad S, Moreno-Cencerrado A, Üzülmez O, Promdonkoy B, Toca-Herrera JL
Bacillus thuringiensis Cyt2Aa2 binding on lipid/cholesterol bilayer depends on protein concentration and time
Biochem Biophys Res Commun 492 (2017) 212, DOI: 10.1016/j.bbrc.2017.08.051

Moreno-Flores S, Ortíz R
Motion mechanics of non-adherent giant liposomes with a combined optical and atomic force microscope
J Phys D: Appl Phys 50 (2017) 435401, DOI: 0.1088/1361-6463/aa8a50

Damiati S, Kupcu S, Peacock M, Eilenberger C, Zamzami M, Qadri I, Choudhry H, Sleytr UB, Schuster B Acoustic and hybrid 3D-printed electrochemical biosensors for the real-time immuno-detection of liver cancer cells (HepG2).
Biosens Bioelectron 94 (2017) 500, DOI: 10.1016/j.bios.2017.03.045

Kameníkova M, Furtmüller PG, Klacsová M, Lopez-Guzman A, Toca-Herrera JL, Vitkovská A, Devínsky F, Muaji P, Nagy M
Influence of quercetin on the interaction of gliclazide with human serum albumin - Spectroscopic and docking approaches
Luminiscence 32 (2017) 1203, DOI: 10.1002/bio.3312

Taczanowska K, Bielanski M, González LM, Garcia-Massó X, Toca-Herrera JL
Analyzing spatial behavior of backcountry skiers in mountain protected areas combining GPS tracking and graph theory
Symmetry 9 (2017) 317, DOI: 10.3390/sym9120317

R. Benítez, V. J. Bolós, J. L. Toca-Herrera
afmToolkit: a R Package for Automated AFM Force-Distance Curves Analysis
The R Journal 9/2 (2017) 291, ISBN: 2073-4859

Conferences, seminars, workshops and schools

AUTHOR: B. Prats-Mateu, N. Gierlinger
TITLE: Cell wall characterization during lignification by Confocal Raman Microscopy
CONFERENCE: 9th PRWAC
PLACE, YEAR: Bali (Indonesia), 2017

AUTHOR: M. Felhofer, B. Prats Mateu, N. Gierlinger
TITLE: Raman imaging to reveal in-situ molecular changes of wood during heartwood formation and drying
CONFERENCE: 19th PRWAC (Pacific Regional Wood Anatomy Conference)
PLACE, YEAR: Denpasar, Bali (Indonesia), 2017

AUTHOR: B. Prats-Mateu, P. Bock, N. Gierlinger
TITLE: Laser induced changes of aromatics during Raman imaging of plant cell walls
CONFERENCE: I Plant Spectroscopy Conference
PLACE, YEAR: Umeå (Sweden), 2017

AUTHOR: P. Bock, B. Prats Mateu, N. Gierlinger
TITLE: Why one laser is not enough – a case study on cinnamaldehydes and the implications on Raman spectroscopy of plant material
CONFERENCE: 1st International Plant Spectroscopy Conference
PLACE, YEAR: Umeå (Sweden), 2017

AUTHOR: V. Golebiewska, N. Gierlinger
TITLE: Unravelling chemistry in context with microstructure of nut shells
CONFERENCE: 1st International Plant Spectroscopy Conference
PLACE, YEAR: Umeå (Sweden), 2017

AUTHOR: M. Felhofer, B. Prats-Mateu, P. Bock, N. Gierlinger
TITLE: Heartwood formation and resin canals in pine
CONFERENCE: 1st International Plant Spectroscopy Conference
PLACE, YEAR: Umeå (Sweden), 2017

AUTHOR: N. Gierlinger
TITLE: Following in-situ hydrophobisation of plant cell walls by Raman imaging
CONFERENCE: 253rd ACS meeting, “Developments in the fields of Celluloses and Lignocelluloses: In Honor of Dr. Rajai Atalla”
PLACE, YEAR: San Fransisco (USA), 2017

AUTHOR: N. Gierlinger
TITLE: Raman scattering and scanning probe approaches on biological materials: principles & prospects
CONFERENCE: Seminar at Institut für Physik
PLACE, YEAR: Montanuniversität Leoben (AUSTRIA), 2017

AUTHOR: J. L. Toca-Herrera
TITLE: Atomic force microscopy, soft matter and other matters
CONFERENCE: seminar at Institute of Science and Technology (IST)
PLACE, YEAR: Klosterneuburg (Austria), 2017

AUTHOR: J. Iturri
TITLE: Studying Cell Mechanics by means of Atomic Force Microscopy
CONFERENCE: Erasmus+ Programme (Staff Training) Invited Seminar.
PLACE, YEAR: Universidad Complutense de Madrid, Facultad de Veterinaria. Madrid (Spain), 2017

AUTHOR: J. Iturri, A. Moreno-Cencerrado, J. L. Toca-Herrera
TITLE: Investigating Cell-Substrate and Cell-Cell interactions by means of Single-Cell-Probe Force Microscopy
CONFERENCE: NanoSpain 2017conference
PLACE, YEAR: San Sebastian (Spain), 2017

AUTHOR: J. Iturri
TITLE: Studying Cell Mechanics by means of Atomic Force Microscopy
CONFERENCE: Erasmus+ Programme (Teaching mobility) seminar
PLACE, YEAR: Ljubljana (Slovenia), 2017

AUTHOR: J. Iturri, J. Miholich, S. Zemlijc-Jokhadar, J. L. Toca-Herrera
TITLE: Elastomeric PDMS stiffness influence on adhesion, culture and mechanics of endothelial cells
CONFERENCE: Liquids 2017 conference
PLACE, YEAR: Ljubljana (Slovenia), 2017

AUTHOR: A. Moreno-Cencerrado, S. Tharad, T. Bogataj, J. Iturri, B. Promdonkoy, C. Krittanai, J. L. Toca-Herrera
TITLE: State of the art of the interaction between cytolytic proteins and lipid-cholesterol bilayers
CONFERENCE: Liquids 2017 conference
PLACE, YEAR: Ljubljana (Slovenia), 2017

AUTHOR: J. Iturri, A. Moreno-Cencerrado, J. L. Toca-Herrera
TITLE: Atomic Force Microscopy as a precision tool to study cell mechanics and adhesion
CONFERENCE: Cell Physics 2017 conference
PLACE, YEAR: Saarbrücken (Germany), 2017

AUTHOR: J. Iturri
TITLE: Atomic Force Microscopy as a tool for studying Cell (and Cell Scaffold) mechanics
CONFERENCE: NanoBio&Med 2017 conference
PLACE, YEAR: Barcelona (Spain), 2017

AUTHOR: S. Tharad, A. Moreno-Cencerrado, B. Prodonkoy, J. L. Toca-Herrera
TITLE: Membrane disruption of action of Bacillus thuringiensis cytolytic toxin (Cyt2Aa2) at low protein concentration studied by AFM and QCM-D
CONFERENCE: 9th ÖGMBT annual meeting
PLACE, YEAR: Innsbruck (Austria), 2017.

AUTHOR: A. Moreno-Cencerrado, J. Iturri, J.L. Toca-Herrera
TITLE: Bacterial proteins in real-time: An atomic force microscopy and quartz crystal microbalance with dissipation study
CONFERENCE: 31st ECIS Conference (European Colloid and Interface Society)
PLACE, YEAR: Madrid (Spain), 2017

AUTHOR: K. Taczanowska, A. Zieba, C. Brandenburg, A. Muhar, H. Preisel, J. Hibner, B. Latosinska, R. Benítez, V. Bolos, J. L. Toca-Herrera, S. Ziobrowski
TITLE: Simultaneous use of several monitoring techniques to measure visitor load, spatio-temporal distribution and social characteristics of
tourists – a case study of a cable car area in the Carpathian Mountains, Tatra National Park
CONFERENCE: EGU General Assembly 2017 (European Geosciences Union)
PLACE, YEAR: Vienna (Austria), 2017

AUTHOR: J.L. Toca-Herrera
TITLE: Atomic force microscopy, what else?
CONFERENCE: Frontiers in Materials Science 2017
PLACE: Greifswald (Germany), 2017

3. Ongoing projects, national and international collaborations, and student supervision

Accepted / Ongoing projects

- "S-layer directed nanoscale fluid mechanics", Air Force Office of Scientific Research (AFOSR), Agreement award FA9550-15-1-0459,
  Dietmar Pum (PI), Uwe B. Sleytr (Co-PI), and Jose-Luis Toca-Herrera (Co-PI)
- "Scattering and tapping on soft, hard, open nuts", ERC-consolidator grant SCATAPNUT, Notburga Gierlinger (PI)
- "Plant surfaces and Interfaces: Lignin, Suberin and Cutin", START-Project Y728-B16 SURFINPLANT (Austrian Science Fund, FWF), Notburga Gierlinger (PI)
- "Meteoriten Chemie und Vergleich mit Kometendaten von Rosetta", FWF-Projekt (P 26871 - N20), Kurt Varmuza (PI, TU-Vienna), Notburga Gierlinger (Co-author)
- „S-layer recrystalization though hydrophobic/hydrophilic nanoprotrusions" FWF-projekt (P29562-N28), Jose L. Toca-Herrera (PI), Dietmar Pum (co-author)
- "Shed new light on heartwood formation" DOC-Programme [24763] from the Austrian Academy of Sciences

National / International collaborations

- Dr. Natalia Baranova, IST, Austria
- Prof. Peter Lieberzeit, Univ. of Vienna, Inst. of Anal. Chem., Vienna, Austria
- Prof. Carole C. Perry, Nottingham Trent University, Nottingham, UK
- Dr. Rafael Benítez, Univ. of Extremadura, Dept. of Mathematics. Spain
- Dr. Luis Millán González, Univ. of Valencia, Dept. of Physical Education and Sport, Spain
- Dr. Chartchai Krittanai, Mahidol University, Institute of Molecular Biosciences, Thailand
- Prof. M. Schneider, Institute biopharmacy and pharmaceutical technology, University of Saarland
- Dr. Maria Vivanco, CICbioGUNE, Spain
- Prof. Longjian Xue, Wuhan University, China
- Dr. Felipe Ortega, Universidad Complutense, Madrid, Spain
- Prof. Ronald F. Ziolo, CIQA – Conacyt, Mexico
- Dr. Spela Zemlijc. University of Ljubjana, Slovenia
- Prof. Hajo Haase / Dr. Claudia Keil, TU-Berlin, Germany
- Dr. Malou Henriksen. CICbiomaGUNE, Spain
- Dr. Anders Lundgren, Chalmers University, Sweden
- Prof. Ingo Burgert, ETH Zurich, Switzerland
- Dr. Michaela Eder, Max Planck Institute of Colloids and Interfaces, Potsdam
- Prof. Anna de Juan, Chemometrics group, University of Barcelona, Diagonal 645, 08028 Barcelona, Spain
- Yaseen Mottiar, Prof. Shawn D Mansfield, University of British Columbia, Forest Sciences Centre 4030, 2424 Main Mall, Vancouver, BC V6T 1Z4, Canada
- Prof. Gilbert Neuner, University of Innsbruck, Institute of Botany, Unit Functional Plant Biology, Sternwartestr. 15, 6020 Innsbruck, Austria
- A.o. Univ. Prof. Ursula Lütz-Meindl, University of Salzburg, Cell Biology and Physiology Department, 5020 Salzburg, Austria
- Prof. Wolfgang Gindl, Institute for Wood technology and Renewable materials, University of Natural Resources and Life Sciences, Vienna, Austria

Student supervision

PhD

1. Alberto Moreno Cencerrado: Proteins at (soft) interfaces
2. Elham Ghorbani Gorji: Resveratrol milk proteins interactions
3. Maria Sumarokova: Mechanical and adhesion properties of protein thin films
4. Zuzana Vanekova (Comenius Univ. Bratislava): Charaterization of protein interactions with calorimetry and fluorescence (exchange grant from ÖEAD)
5. Sonia Krysiak (AGH-Krakow): Surface and mechanical properties of fluorescence lipid layers (WTZ exchange project from ÖEAD)
6. Eva Sanchez (Univ. Basque Country): Miscibility, Interactions and Antimicrobial Activity of Poly(ε-caprolactone)/Chloramphenicol Blends (grant of the Regional Basque Government)
7. Batirtze Prats Mateu (START): Raman-imaging and Atomic force microscopy approaches to reveal microchemistry and nanostructure of biological materials
8. Peter Bock (START/ERC): Raman and IR spectroscopy on plant aromatics to gain a better understanding of secondary cell walls
9. Nannan Xiao (ERC): From soft to hard material: Understanding nut shell development on the micro- and nanoscale
10. Nadia Sassani (START): Lignin and cutin distribution and composition on the microscale to understand waterproofing and protection of plants
11. Carmen Texeira (Lincoln University): Phenological development of subterranean clover cultivars (Kathleen Spragg Agricultural Research Trust)

MSc/Diploma/Training/Erasmus

1. Andreas weber: Mechanical properties of elastomeric polydimethylsiloxane
2. Piet Mitjen (Erasmus Program, Gent University) : Polymer viscoleasticity
3. Christoph Pötcher (collaboration with LIST-company): Microspectroscopy on Mahagony veneers: a way to understand discolorations?
4. Leif Löher (Erasmus Program, TU-Berlin, Germany): cell mechanics
5. Damir Begic (CEEPUS program, University of Sarajevo, Bosnia-Herzegoniva): Polymer capsules in drug delivery

BSc

1. Karolina Peter: Harte Nuss und Hartholz, ein Vergleich der Festigungsgewebe auf Mikroebene
2. Michael Pilgerstorfer: Micropatterning and release

Prizes

Klaus Fischer – Innovationspreis für Technik und Umwelt for the Masterthesis “RAMAN imaging to reveal in-situ molecular changes of wood during heartwood formation and drying“
Place, Year: BOKU Vienna, May 11, 2017

4. Miscelanea

Summer School of the Institute for Biophysics (DNBT, BOKU Vienna), Bad Tatzmannsdorf, Austria; 12th-14th September 2017)

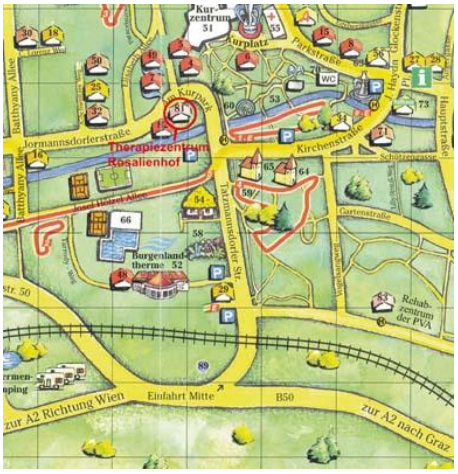

Participants:

Amsatou ANDORFER-SARR, Peter BOCK, Andreas BREITWIESER, Martin FELHOFER, Jacqueline FRIEDMANN, Notburga GIERLINGER, Radostina GIORGIEVA (La Charite, Berlin), Violetta GOLEBIEWSKA, Michael HANDLER (Univ. Innsbruck), Jagoba Jon ITURRI, Dieter JÄGER, Alberto MORENO-CENCERRADO, Batirtze PRATS MATEU, Dietmar PUM, Uwe B. SLEYTR, Iris STRUBE, José-Luis TOCA-HERRERA, Öykü ÜZÜLMEZ, Andreas WEBER

Programm

Tuesday – 12 | 09 | 2017
14.00-15.15 h
- Opening of the Biophysics Sommer School: José L. Toca-Herrera
Session 1 Chair: Dietmar Pum
(Talk 1) Jagoba Jon Iturri
(Talk 2) Batirtze Prats-Mateu
Coffee break: 15 minutes
15:30-16:20 h
(Talk 3) Martin Felhofer
(Talk 4) Alberto Moreno-Cencerrado
16:30 – 17:15 h
POSTER Session

Wednesday – 13 | 09 | 2017
9.15-10.15 h
Session 2 Chair: Notburga Gierlinger
(Talk 5) Radostina Giorgieva
(Talk 6) Peter Bock
(Talk 7) Violetta Golebiewska
Coffee break: 15 minutes
10.30-11.45 h
Session 3 Part I Chair: Jagoba Jon Iturri
(Talk 8) Andreas Weber
(Talk 9) Öykü Üzülmez
(Talk 10) Michael Handler
Lunch break and relaxing time

14.30-15.20 h
Session 3 Part II Chair: Jagoba Jon Iturri
(Talk 11) Andreas Breitwieser
(Talk 12) Dietmar Pum
Coffee break: 15 minutes
15:35-16:30 h
José L. Toca-Herrera: CLOSING NOTES - Round table

Thursday – 14 | 09 | 2017
9.30 h - 11.25 h: Brain storming and lightening (optional)
11.30 h - 14.00 h: Lunch break
14.30 h: Departure to Vienna